and differentiate into osteoclasts in the presence of M-CSF and RANKL. In this study, we investigated the role of M-CSF in osteoclastogenesis in this system. We found that bone marrow macrophages also produce OPG and that this OPG production was suppressed by M-CSF. These results suggest that M-CSF increases the sensitivity of osteoclast progenitors to RANKL by down-regulation of their OPG production.

2. Results

2.1. Phenotypic analysis of bone marrow macrophages

Mouse bone marrow cells were cultured with recombinant human (rh)M-CSF (100 ng/ml) for 4 days, and adherent cells (bone marrow macrophages; BMMs) were analyzed for expression of various surface antigens by flowcytometry. Essentially all BMMs were positive for specific surface markers for macrophages, Mac-1 (96.9%) and CD115 (M-CSF receptor, c-fms) (95.3%) (Fig. 1B and C). Contour plot analysis showed Mac-1-positive BMMs were homogenous in cell size (Fig. 1A). All BMMs also expressed another macrophage marker, F4/80 (data not shown) while they expressed another macrophage marker, CD14, weakly (Fig. 1D). However, BMMs expressed no specific markers for granulocytes (Gr-1/Ly-6G) (Fig. 1E), NK cells (CD122) (Fig. 1F) and T cells (CD3) (Fig. 1G). Histochemical analysis of 1×10^6 BMMs detected no alkaline phosphatase activity in BMMs. Reverse transcription-polymerase chain reaction (RT-PCR) with total RNA from BMMs showed no expression of calcitonin receptor mRNA (data not shown).

2.2. Phagocytotic activity and osteoclastogenic ability of BMMs

BMMs (Fig. 2A) showed phagocytotic activity (Fig. 2B) but not tartrate-resistant acid phosphatase (TRAP) activity (data not shown). In the presence of rhM-CSF (25 ng/ml), BMMs remained TRAP-negative mononuclear cells after 4 days of culture (Fig. 2C), but in the presence of both rhM-CSF (25 ng/ml) and recombinant human soluble (rhs) RANKL (25 ng/ml), they differentiated into TRAP-positive multinucleated osteoclasts (Fig. 2D). In the presence of rhsRANKL (25 ng/ml), rhM-CSF at 5–50 ng/ml induced osteoclastogenesis of BMMs dose-dependently after 4 and 7 days of culture (Fig. 3A and B).

2.3. Suppression of expression of OPG mRNA and secretion of OPG by M-CSF

Fig. 4A shows the effect of rhM-CSF on OPG mRNA expression in BMMs. Expression of OPG mRNA in BMMs increased with time in culture without rhM-CSF, and was suppressed in the presence of rhM-CSF (25 ng/ml). The amount of OPG secreted in medium was also markedly suppressed by rhM-CSF (25 ng/ml) when expressed as pg OPG/10^4 cells (Fig. 4B-1). The number of viable BMMs after 4 or 7 days of culture was much less in the absence of rhM-CSF than in the presence of rhM-CSF (Fig. 4B-2). However, the concentration of OPG in medium was also decreased by rhM-CSF; average OPG concentrations in medium in culture without rhM-CSF vs. those with rhM-CSF were 236 vs. 111 pg/ml during days 0–4 and 999 vs. 444 pg/ml during days 5–7. The amounts of nitrite plus nitrate in medium on days 0–4 and 5–7 with or without rhM-CSF (25 ng/ml) were below the limit of detection, i.e., 10 μM.

The inhibitory effects of M-CSF on the expression of OPG mRNA was dose-dependent (Fig. 5A), with significant effects on both expression of OPG mRNA and secretion of OPG observed at 10 ng/ml when examined in culture for 4 days (Fig. 5A and B-1). The number of viable BMMs increased dose-dependently (Fig. 5B-2), but the OPG concentration in medium was also decreased in the presence of rhM-CSF. Average OPG concentrations in the medium in the absence of rhM-CSF and in the presence of rhM-CSF at 10, 30 and 60 ng/ml were 120, 49, 52 and 32 pg/ml, respectively. rhsRANKL (25 ng/ml) did not affect OPG mRNA expression in BMMs with or without rhM-CSF (25 ng/ml) (data not shown).

To confirm the production of OPG in BMMs, we performed double-staining analysis of OPG and CD115 (Fig. 6). The results showed that OPG mRNA was expressed in CD115-positive cells.

2.4. Reversible effects of M-CSF on secretion of OPG by BMMs

BMMs were first cultured in the absence of rhM-CSF for 4 days and subsequently in the presence or absence of rhM-CSF (60 ng/ml) for 4 days. The delayed addition of rhM-CSF inhibited the secretion of OPG by BMMs expressed as pg OPG/10^4 cells (Fig. 7A) or a concentration in medium in spite of a difference in viable cell number (Fig. 7B). Average OPG concentrations in the medium in the presence and absence of rhM-CSF were 1992 and 3192 pg/ml, respectively.

We also examined whether the inhibition of OPG secretion by rhM-CSF (60 ng/ml) was reversible by culturing BMMs with rhM-CSF for 4 days, removing rhM-CSF and further culturing for 4 days. The removal of rhM-CSF increased the secretion of OPG by BMMs expressed as pg OPG/10^4 cells (Fig. 7A) or a concentration in medium in spite of a difference in viable cell number (Fig. 7B) although the extent of recovery of OPG secretion was small. Average OPG concentrations

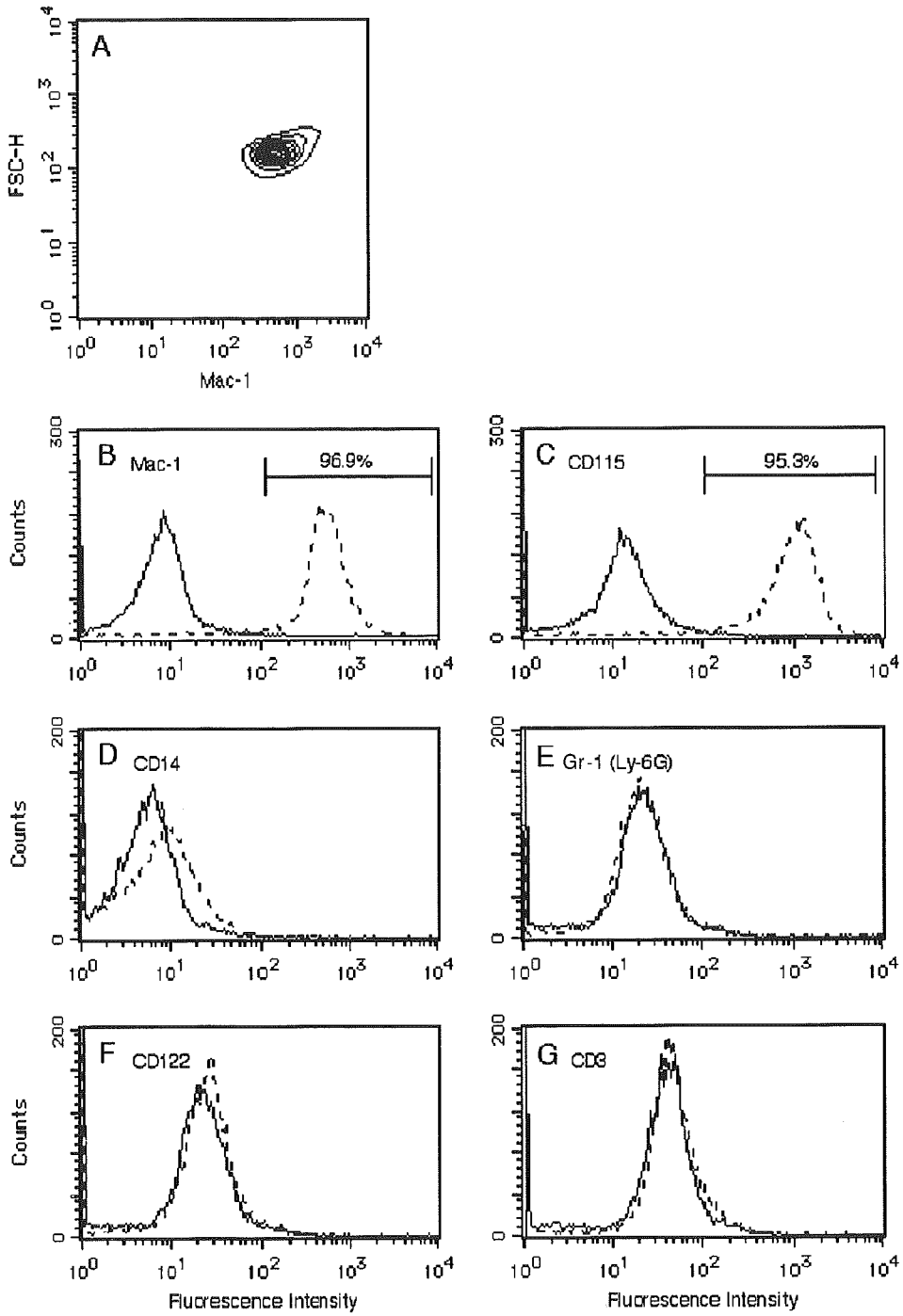

Fig. 1. Phenotypic analysis of BMMs. Bone marrow cells were cultured with rhM-CSF (100 ng/ml) for 4 days, and adherent cells (BMMs) were analyzed for expression of Mac-1 (A, B), CD115 (C), CD14 (D), Gr-1 (E), CD122 (F) and CD3 (G) by flowcytometry. The top figure shows a contour plot analysis for Mac-1 and forward scatters (FSC), and the other figures show histograms for various surface antigens. Dashed and solid lines show profiles with and without antibody, respectively.

in medium in the presence and absence of rhM-CSF were 242 and 653 pg/ml.

2.5. Expression of RANK mRNA in BMMs

Analysis of RANK mRNA showed that BMMs expressed RANK mRNA, and this expression was not significantly affected by M-CSF at concentrations up to 60 ng/ml (Fig. 8).

2.6. Effect of OPG on osteoclastogenesis

To examine the effect of OPG on osteoclastogenesis, BMMs were cultured with rhM-CSF (25 ng/ml),

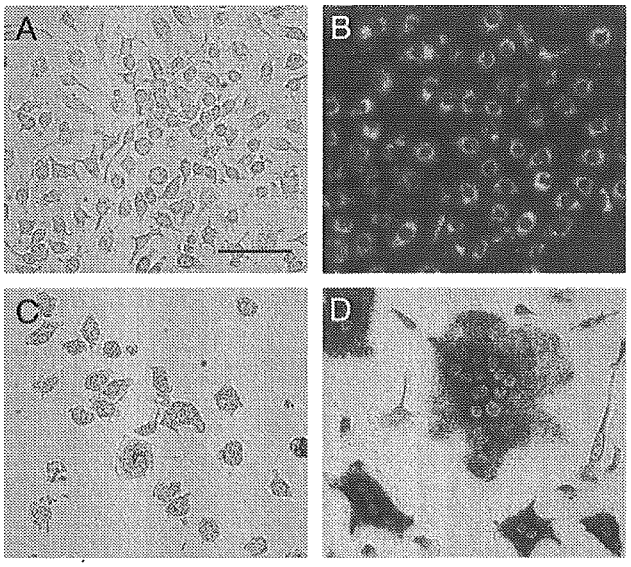

Fig. 2. Phagocytotic and osteoclastogenic activities of BMMs. Bone marrow cells were cultured with rhM-CSF (100 ng/ml) for 4 days, and phagocytotic and osteoclastogenic activities of adherent cells (BMMs) were examined. The phagocytotic activity was assayed by phagocytosis of FITC-labeled beads. The osteoclastogenic activity was estimated by culturing BMMs for 4 days with rhM-CSF (25 ng/ml) and rhsRANKL (25 ng/ml) and by staining for TRAP. (A) BMMs. (B) BMMs showing phagocytosis of FITC-labeled beads. (C) BMMs cultured in the presence of rhM-CSF only, showing no TRAP-positive osteoclasts. (D) BMMs cultured in the presence of rhM-CSF and rhsRANKL, showing TRAP-positive multinucleated osteoclasts. Magnifications of Fig. A–D are same (bar: 50 μm).

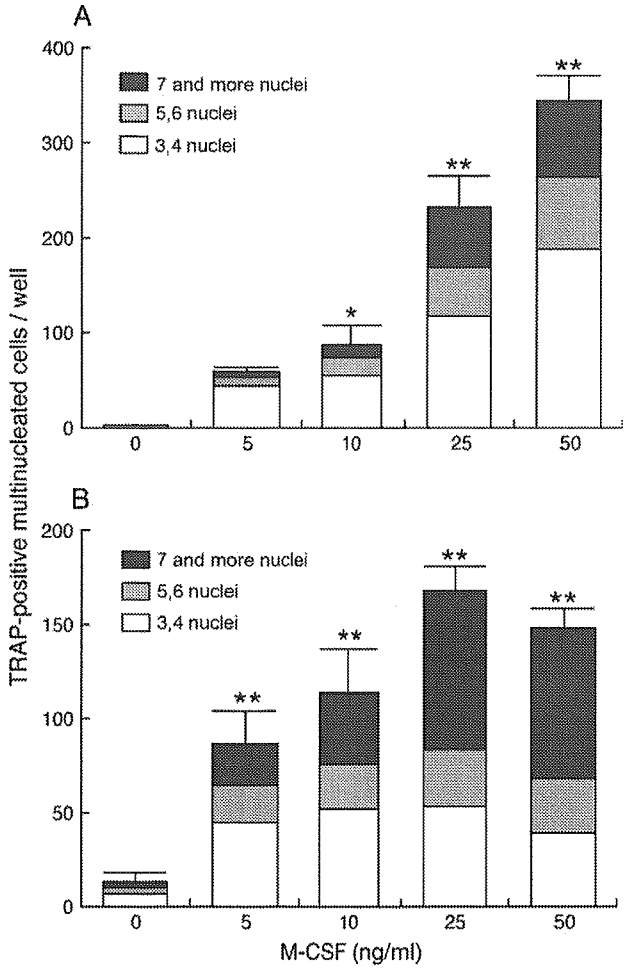

Fig. 3. Dose-dependent effects of M-CSF on the osteoclastogenesis of BMMs. BMMs were cultured with various concentrations of rhM-CSF in the presence of rhsRANKL (25 ng/ml) for 4 days (A) or 7 days (B), and stained for TRAP. TRAP-positive cells with 3 or 4 nuclei, 5 or 6 nuclei or 7 and more nuclei were counted. Each bar represents a mean + SE of total cell numbers for 5 samples. $^{**}P < 0.01$ and $^{*}P < 0.05$, significant difference from values for culture without rhM-CSF (0 ng/ml) by Bonferroni multiple comparison test.

rhsRANKL (25 ng/ml) and 1–100 ng/ml of recombinant mouse (rm) OPG for 4 or 7 days, and analyzed for the formation of multinucleated TRAP-positive osteoclasts. OPG was found to inhibit osteoclastogenesis dose-dependently (Fig. 9).

3. Discussion

Essentially all BMMs used in this study were positive for macrophage surface markers, Mac-1 (96.9%), CD115 (M-CSF receptor, c-fms) (95.3%) and F4/80 (100%), and showed phagocytotic activity, indicating that they were macrophages. Treatment of these cells with M-CSF and sRANKL induced TRAP activity with the formation of multinucleated osteoclasts. These results indicated that BMMs used were likely to have been osteoclast progenitors, as reported by Kobayashi et al. [13].

BMMs used in this study were adherent cells formed when bone marrow cells were incubated with M-CSF for 4 days. Among bone marrow cells, stromal cells, osteoblasts and osteoclasts have been shown to produce OPG [9,14]. Stromal cells and osteoblasts express alkaline phosphatase [15], and osteoclasts TRAP. However, BMMs used in this study were negative for both alkaline phosphatase and TRAP, showing no contamination of stromal cells, osteoblasts and osteoclasts. On the other hand, BMMs were positive for both CD115, macrophage marker, and OPG, indicating that BMMs themselves produce OPG. OPG mRNA is expressed in various tissues such as lung, heart, kidney, liver, thyroid, spinal cord, brain and placenta, in addition to bone marrow stromal cells, osteoblasts and osteoclasts [9,14,16]. Moreover, endothelial cells, aorta smooth muscle cells, fibroblasts, T and B lymphocytes, dendritic cells and various tumor cell lines have been reported to express OPG mRNA [9,12,14]. The present results show that BMMs are an additional potential source of OPG.

The removal of M-CSF increased the secretion of OPG by BMMs but the extent of recovery of the OPG secretion was small. This may be partly due to the

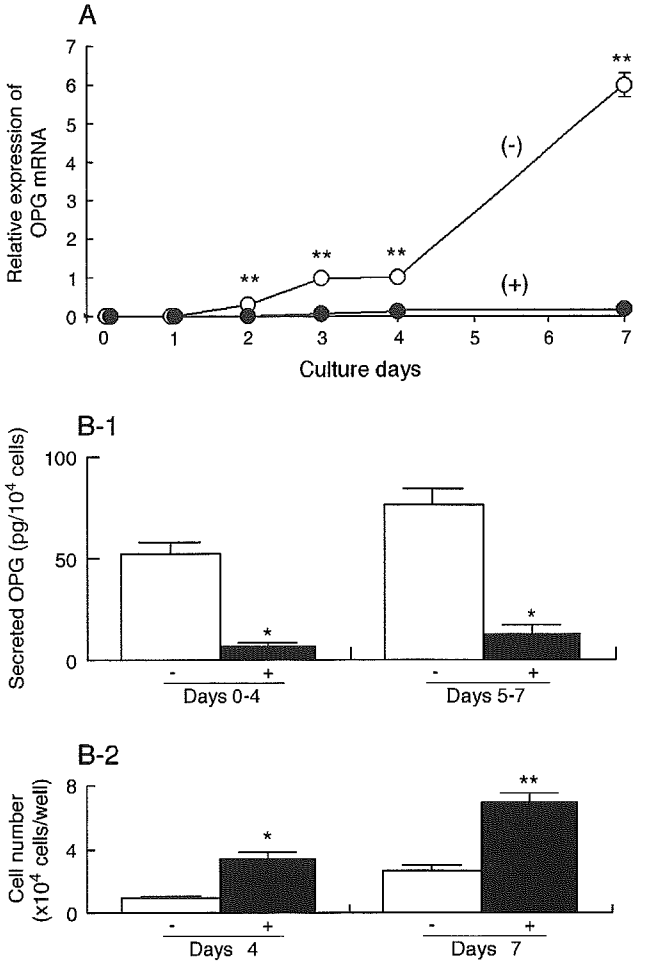

Fig. 4. Time-course analysis of effects of M-CSF on the expression of OPG mRNA and the secretion of OPG by BMMs. BMMs were cultured with (+) or without (−) rhM-CSF (25 ng/ml) for 7 days. (A) OPG and GAPDH mRNAs were estimated on different days by real-time PCR. OPG mRNA values were normalized to GAPDH mRNA values and expressed relative to OPG mRNA expressed in control cells without M-CSF on day 4. Each point represents a mean ± SE for 5 samples. $^{**}P < 0.01$, significant difference from values for culture with rhM-CSF on the same day by Student's t-test. (B) OPG secreted into medium during days 0–4 or days 5–7 (B-1) and viable cell number on days 4 and 7 (B-2). Each point represents a mean + SE for 5 samples. $^{**}P < 0.01$ and $^{*}P < 0.05$, significant difference from values for culture without rhM-CSF by Student's t-test.

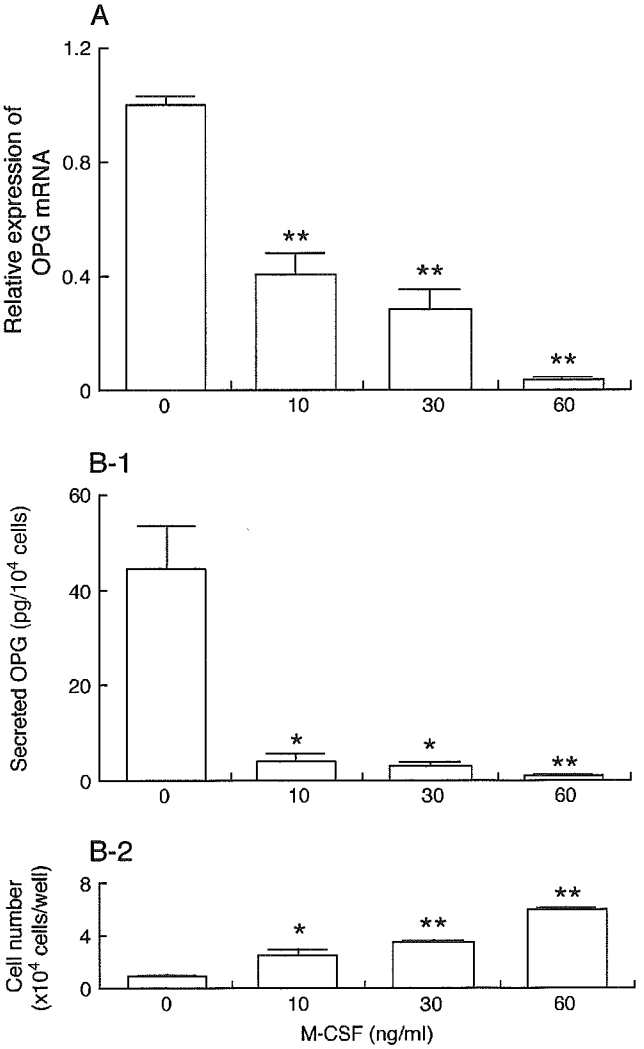

Fig. 5. Dose-dependent inhibition of expression of OPG mRNA and secretion of OPG by M-CSF. BMMs were cultured with various concentrations of rhM-CSF for 4 days, and analyzed for OPG mRNA and secreted OPG. (A) Effect of M-CSF on OPG mRNA expression. OPG mRNA expression was normalized to GAPDH mRNA expression and expressed relative to OPG mRNA expressed in control cells without M-CSF. (B) Effect of M-CSF on OPG secretion (B-1) and viable cell number (B-2). Each bar represents a mean + SE for 5 samples. $^{**}P < 0.01$ and $^{*}P < 0.05$, significant difference from values for culture without M-CSF by Bonferroni multiple comparison test.

sustaining intracellular effects of M-CSF after deprivation of M-CSF in terms of OPG production.

In the in vitro system of osteoclastogenesis using BMMs, 25 ng/ml of rhM-CSF seem to be its adequate but not pharmacological concentration for induction of osteoclastogenesis in the presence of rhsRANKL (25 ng/ml) (Fig. 3) and rhM-CSF at this concentration suppressed the OPG production in BMMs markedly. OPG is a decoy receptor which blocks binding of RANKL to RANK [8–12]. Consistently, we observed that OPG at 1 ng/ml inhibited osteoclastogenesis of BMMs induced by rhM-CSF (25 ng/ml) and rhsRANKL (25 ng/ml). Furthermore, we observed that in the absence of M-CSF, the average concentration of OPG in medium after 7 days of culture was more than 1 ng/ml (Fig. 4; average OPG concentrations during days 0–4 and days 5–7 were 236 and 998 pg/ml, respectively) suggesting that without M-CSF, BMMs secrete a relatively large amount of OPG which may interfere with the action of RANKL, thus suppressing osteoclastogenesis. Therefore, the suppression by M-CSF of the OPG production in osteoclast progenitors seems to play a role in increasing the sensitivity of osteoclast progenitors to RANKL at least in this in vitro system of osteoclastogenesis.

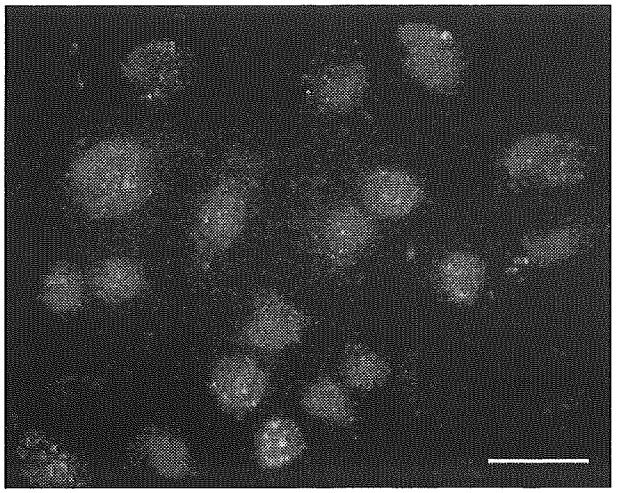

Fig. 6. Analysis of CD115 and OPG in BMMs by double staining. BMMs were cultured without rhM-CSF (25 ng/ml) for 7 days, and stained with FITC-labeled anti-CD115 (green) and rhodamin-labeled anti-OPG (red) antibodies. Bar: 20 μm.

In osteoclastogenesis mediated by bone marrow stromal cells or osteoblasts, several hormones and cytokines, such as parathyroid hormone, glucocorticoid, vitamin D_3, prostaglandin E_2, IL-1, TNF-α, IL-11, have been shown to stimulate osteoclastogenesis by increasing

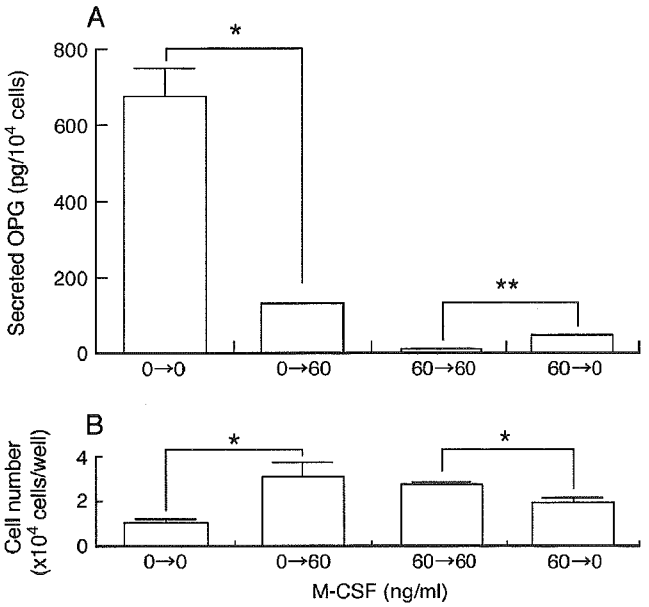

Fig. 7. Effects of the delayed addition and removal of M-CSF on OPG secretion. In one experiment, BMMs were first cultured without rhM-CSF for 4 days, then with (0 → 60) or without (0 → 0) rhM-CSF (60 ng/ml) for further 4 days and analyzed for OPG in medium. In another experiment, BMMs were first cultured with rhM-CSF (60 ng/ml) for 4 days, then with (60 → 60) or without (60 → 0) rhM-CSF (60 ng/ml) for further 4 days, and analyzed for OPG in medium. (A) Secreted OPG in medium during the second culture. (B) Number of viable cells at the end of culture. Each bar represents a mean + SE for 5 samples. $^{**}P < 0.01$ and $^{*}P < 0.05$, significant difference by Student's t-test.

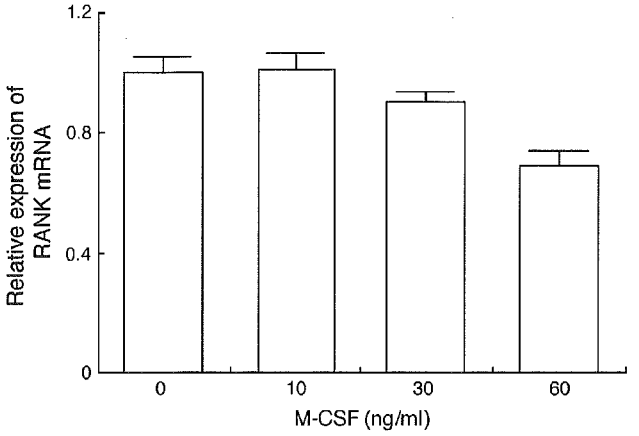

Fig. 8. Effect of M-CSF on expression of RANK mRNA. BMMs were cultured with various concentrations of rhM-CSF for 4 days, and analyzed for RANK and GAPDH mRNAs by real-time PCR. RANK mRNA expression was normalized to GAPDH mRNA expression and expressed relative to RANK mRNA expressed in control cells without M-CSF. Each bar represents a mean + SE for 5 samples. There were no significant differences among values at various concentrations of rhM-CSF by Bonferroni multiple comparison test.

relative expression of RANKL to OPG in stromal cells or osteoblasts [9,10,12]. The present in vitro study showed that osteoclast progenitors themselves produce OPG, and that M-CSF, the other obligatory requirement for osteoclastogenesis besides RANKL, suppresses their OPG production in favor of osteoclastogenesis. However, some cytokines, such as TNF-α, IL-6 and IL-11, exert effects directly on osteoclast progenitors to induce osteoclastogenesis in the presence of M-CSF by a RANKL-independent mechanism [13,17–19]. Therefore, the inhibitory effect of M-CSF on the OPG production by osteoclast progenitors does not appear to be essential for RANKL-independent osteoclastogenesis although it is important for RANKL-dependent osteoclastogenesis.

Wang et al. [20] have reported that the OPG production by bone marrow stromal cells is increased by nitric oxide. Therefore, the involvement of nitric oxide in the inhibitory effect of M-CSF on the OPG production by BMMs was examined. However, the amount of metabolites of nitric oxide, nitrite plus nitrate, in medium was too small to assess a role of nitric oxide in the OPG production by BMMs. Further studies with nitric oxide donor or using an inducible nitric oxide synthase (NOS) knockout mouse are desired.

M-CSF exerted no significant effect on RANK mRNA expression in BMMs. Arai et al. [21] reported that M-CSF induced RANK expression in c-kit-positive, c-fms-positive and Mac-1-negative bone marrow mononuclear osteoclast progenitors which did not express RANK. Cappellen et al. [22] also reported that M-CSF up-regulated expression of RANK mRNA in bone marrow mononuclear osteoclast progenitors which expressed little mRNAs of c-fms and RANK. Bone

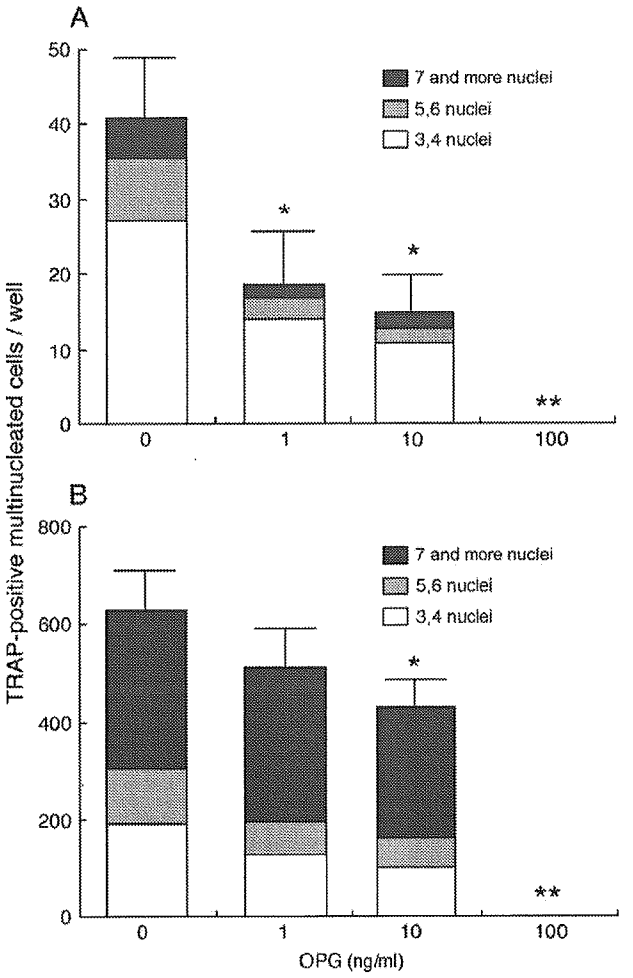

Fig. 9. Effect of OPG on osteoclastogenesis of BMMs. BMMs were cultured with rhM-CSF (25 ng/ml) and rhsRANKL (25 ng/ml) in the presence of various concentrations of rmOPG for 4 days (A) or 7 days (B), and stained for TRAP. TRAP-positive cells with 3 or 4 nuclei, 5 or 6 nuclei or 7 and more nuclei were counted. Each bar represents a mean + SE of total cell numbers for 5 samples. $^{**}P < 0.01$ and $^{*}P < 0.05$, significant difference from values for culture without OPG (0 ng/ml) by Bonferroni multiple comparison test.

marrow mononuclear osteoclast progenitors used in the studies of Arai et al. [21] and Cappellen et al. [22] were not treated with M-CSF during preparation of osteoclast progenitors. However, BMMs used in this study had been exposed to rhM-CSF (100 ng/ml) for 4 days, and were Mac-1-, c-fms- and CD14-positive and expressed RANK mRNA. As shown by Takeshita et al. [23] and Cappellen et al. [22], M-CSF plays roles of a differentiation factor as well as a growth factor for osteoclast early progenitors. Therefore, the difference in the effect of M-CSF on RANK expression between studies of Arai et al. [21] and Cappellen et al. [22], and ours seems to be derived from different stages of differentiation of osteoclast progenitors used in the study.

In conclusion, the present study shows that M-CSF suppresses the production of OPG in BMMs in vitro, which, if occurs in vivo, indicates that M-CSF may act to increase the sensitivity of osteoclast progenitors to RANKL.

4. Materials and methods

4.1. Materials

Recombinant human soluble (rhs) RANKL was purchased from PeproTech (London, UK), and recombinant mouse (rm) OPG from R & D Systems (Minneapolis, MN). Biotinylated rat anti-mouse CD115 (c-fms) antibody, FITC-labeled rat anti-mouse Mac-1 antibody, Cychrome-labeled rat anti-mouse CD3 antibody, PE-labeled rat anti-mouse CD14, PE-labeled rat anti-mouse CD122 and Gr-1 (Ly-6G) antibodies, Cychrome-conjugated streptavidin, FITC-conjugated avidin and Fc-block were purchased from BD Biosciences (San Jose, CA), rabbit anti-mouse OPG antibody and rhodamin-conjugated anti-rabbit IgG from Santa Cruz Biotechnology (Santa Cruz, CA), rat anti-mouse F4/80 antibody from Biomedicals AG (Rheinstrasse, Augst, Switzerland), Fluospheres (FITC-labeled microspheres) from Invitrogen (Carlsbad, CA), and Fast Blue Salt BB and naphthol AS-BI phosphoric acid from Sigma (St. Louis, MO). A mouse OPG enzyme-linked immunosorbent assay (ELISA) kit was purchased from Techne (Minneapolis, MN), a nitrite/nitrate assay kit from Wako (Osaka, Japan), and a leukocyte acid phosphatase kit from Sigma. Recombinant human (rh)M-CSF was kindly provided by Dr. T. Kuhara (Morinaga Milk Industry; Tokyo, Japan).

4.2. Mice

Male Balb/c mice of 7 weeks of age were purchased form Japan SLC (Hamamatsu, Shizuoka, Japan). Mice were kept at 25 °C under controlled light conditions (12 h light/12 h dark), and allowed free access to water and a pellet diet. All experiments conformed to the guidelines for the "Care and Use of Animals" in the Information for Authors Section of the American Journal of Physiology, and were approved by the Animal Care Committee of Hyogo College of Medicine.

4.3. Isolation of bone marrow macrophages

The femurs and tibias of 7-week-old mice were aseptically removed and dissected free of adhering tissues. The bone ends were cut off with scissors and the marrow cavity was flushed with α-Minimal Essential Medium (α-MEM) by slowly injecting at one end of the bone using a sterile needle to collect bone marrow cells. These cells were washed with α-MEM, and red blood cells contained were burst by treatment with 155 mM

NH_4Cl, pH 7.3, containing 14.2 mM $NaHCO_3$ and 1 mM ethylenediaminetetraacetic acid disodium salt (EDTA). Cells were washed with Ca^{++}, Mg^{++}-free Dulbecco's phosphate-buffered saline, pH 7.4 (PBS), and cultured at 5×10^6 cells/10 cm tissue culture dish in 10 ml of α-MEM containing 10% fetal bovine serum (FBS), 100 IU/ml penicillin G and 100 μg/ml streptomycin with rhM-CSF (100 ng/ml). Floating cells were removed and attached cells were harvested by treatment with PBS containing 0.02% EDTA and used as bone marrow macrophages (BMMs).

4.4. Flowcytometry

BMMs were suspended in ice-cold PBS containing 2% FBS (PBS–FBS). Cells were incubated in Fc-block diluted with PBS (1:25 dilution) on ice for 30 min and subsequently with FITC-labeled Mac-1, Cychrome-labeled CD3, PE-labeled Gr-1, PE-labeled CD14, PE-labeled CD122 or biotinylated CD115 antibody (1:100 dilution for each antibody) on ice for 30 min. When cells were incubated with biotinylated CD115 antibody, cells were washed with PBS–FBS and further incubated with Cychrome-conjugated streptavidin (1:200 dilution) on ice for 30 min. Cells were then washed with PBS–FBS and analyzed by an FACS Calibur flowcytometer (Becton Dickinson; Mountain View, CA).

4.5. Alkaline phosphatase staining

BMMs obtained as described above were collected on glass slides using a Shandon Cytospin 3 cytocentrifuge (Thermo Electron Corp.; Wltham, MA) and fixed in 3.7% formaldehyde in methanol for 30 s at 4 °C. The cells were then incubated with a freshly prepared alkaline phosphatase substrate solution (0.2 M Tris–HCl buffer, pH 9.2, containing 1 mg/ml Fast Blue Salt BB and 1 mg/ml naphthol AS-BI phosphoric acid) for 60 min at room temperature. The reaction was terminated by removal of the substrate solution and washing with water. After counterstaining with hematoxylin, 1×10^6 cells were examined for the expression of alkaline phosphatase activity.

4.6. Reverse transcription-polymerase chain reaction (RT-PCR)

Total RNA was extracted from BMMs in dishes using TRIZOL reagent (Invitrogen; Carlsbad, CA). First strand cDNA was synthesized from 1 μg of total RNA with a random primer and Superscript II Reverse Transcriptase (Invitrogen), and an aliquot of the cDNA was subjected to PCR amplification with EX *Taq* polymerase (Takara; Tokyo, Japan) using the following specific PCR primers: a sense primer, 5′-AAGCACAT GTTCCTTACTTA-3′ (1060–1079) and an antisense primer, 5′-ACAAACTGGATCCCCAGCAGGGGCA C-3′ (1663–1688) for the mouse *calcitonin receptor* gene and a sense primer, 5′-GGGTTCCCATAAAGTCACT CTG-3′ (266–287) and an antisense primer, 5′-TCAG TCTATGTCCTGAACTTTGAA-3′ (633–654) for the mouse *β-actin* gene. The PCR conditions were 94 °C for 30 s, 58 °C for 30 s, and 72 °C for 1 min for 35 cycles, with a gene-Amp PCR system 2400 (Perkin–Elmer; Norwalk, CT). The amplified fragments were detected in the expected sizes by ethidium bromide staining in a 1% agarose gel.

4.7. Phagocytotic activity of BMMs

Bone marrow cells obtained as described above were cultured in 96-well plate at 1×10^5 cells/well in 0.2 ml of α-MEM containing 10% FBS with rhM-CSF (100 ng/ml) for 4 days, and adherent cells (BMMs) formed were cultured in α-MEM containing 10% FBS with Fluospheres (1:1000 dilution) for 3 h. After washing with PBS, cells were examined with a fluorescence microscope (Nikon; Tokyo, Japan) and picture analyzer software (AQUACOSMOS) (Hamamatsu Photonics; Hamamatsu, Shizuoka, Japan).

4.8. Tartrate-resistant acid phosphatase (TRAP) staining

BMMs seeded in 96-well plates (1×10^5 cells/well) were cultured in 0.2 ml per well of α-MEM containing 10% FBS with rhM-CSF (25 ng/ml) only, with rhM-CSF (5, 10, 25 or 50 ng/ml) and rhsRANKL (25 ng/ml) or with rhM-CSF (25 ng/ml), rhsRANKL (25 ng/ml) and various concentrations of rmOPG for 4 or 7 days. After culture, cells were fixed and stained for TRAP using a leukocyte acid phosphatase kit. TRAP-positive multinucleated cells were counted as multinucleated osteoclasts.

4.9. Real-time PCR

BMMs were seeded in a 60-mm tissue culture dish (2.5×10^6 cells/dish) and cultured in 5 ml of α-MEM containing 10% FBS with rhM-CSF at various concentrations. Medium was changed after 4 days. Total RNA was extracted using TRIZOL reagent (Invitrogen). First strand cDNA was synthesized from 1 μg of total RNA with a random primer and Superscript II Reverse Transcriptase (Invitrogen). Real-time PCR analysis of mouse OPG, RANK or GAPDH was performed using the real-time PCR kits with an ABI PRISM 7900HT (Applied Biosystems; Foster, CA). The PCR condition was denaturation at 95 °C for 15 s, and annealing and extension at 60 °C for 1 min, for 40 cycles.

4.10. OPG assay

BMMs were seeded in 96-well plates (1×10^5 cells/well) and cultured in 0.2 ml per well of α-MEM containing 10% FBS with rhM-CSF at an indicated concentration for 4, 7 or 8 days. Medium was changed after 4 days. After culture, attached cells were harvested by treatment with PBS containing 0.02% EDTA and viable cells were counted by the trypan blue exclusion test. OPG in medium was determined using a mouse OPG ELISA kit. The sensitivity of the assay was 10 pg/ml, and the intra- and inter-assay coefficients of variation were within 6% and 11%, respectively. The amount of OPG secreted in medium was expressed as pg/10^4 cells.

4.11. Assay of nitrite and nitrate

BMMs were seeded in 96-well plates (1×10^5 cells/well) and cultured in 0.2 ml per well of α-MEM without phenol red (Invitrogen) containing 10% FBS with rhM-CSF (25 ng/ml) for 7 days. The amounts of nitrite plus nitrate in medium on days 0–4 and 5–7 were assayed using a nitrite/nitrate assay kit. The lower limit of an assay of this kit was 10 μM.

4.12. Double-staining of CD115 and OPG

BMMs seeded on Lab-Tec chamber slides (Nalge Nunc Int.; Chester, NY) were cultured in α-MEM containing 10% FBS without rhM-CSF for 7 days, fixed in 4% paraformaldehyde for 1 h and treated in PBS containing 0.2% Triton X100 for 15 min. After incubation with PBS containing 2% bovine serum albumin (BSA) for 30 min at room temperature, BMMs were incubated with biotin-conjugated anti-mouse CD115 antibody (1:100 dilution) and rabbit anti-mouse OPG antibody (1:100 dilution) at 37 °C for 1 h, and subsequently with FITC-conjugated avidin (1:100 dilution) and rhodamin-conjugated anti-rabbit IgG (1:100 dilution) at 37 °C for 30 min. BMMs on slides were mounted in 50% glycerin and examined with a fluorescence microscope (Nikon) and picture analyzer software (ARGUS) (Hamamatsu Photonics).

4.13. Statistical analysis

Data are presented as means ± SE. Data of 3 groups or more were analyzed with Bonferroni multiple comparison test and data of 2 groups were analyzed with Student's *t*-test. A P value less than 0.05 was considered significant.

Acknowledgments

This work was supported in part by a Grant-in-Aid for Researchers, Hyogo College of Medicine, and a Hitec Research Center grant and a Grant for Scientific Research from the Japanese Ministry of Education, Culture, Sports, Science and Technology.

The authors thank Dr. H. Tsutsui, Dr. Y. Yasuda and Ms. H. Takeda for their technical support.

References

[1] Udagawa N, Takahashi N, Akatsu T, Tanaka H, Sasaki T, Nishihara T, et al. Origin of osteoclasts: mature monocytes and macrophages are capable of differentiating into osteoclasts under a suitable microenvironment prepared by bone marrow-derived stromal cells. Proc Natl Acad Sci U S A 1990;87:7260–4.

[2] Hayashi S, Yamane T, Miyamoto A, Hemmi H, Tagaya H, Tanio Y, et al. Commitment and differentiation of stem cells to the osteoclast lineage. Biochem Cell Biol 1998;76:911–22.

[3] Suda T, Takahashi N, Udagawa N, Jimi E, Gillespie MT, Martin TJ. Modulation of osteoclast differentiation and function by the new members of the tumor necrosis factor receptor and ligand families. Endocr Rev 1999;20:345–57.

[4] Jimi E, Nakamura I, Amano H, Taguchi Y, Tsurukai T, Tamura M, et al. Osteoclast function is activated by osteoblastic cells through a mechanism involving cell-to-cell contact. Endocrinology 1996;137:2187–90.

[5] Takahashi N, Udagawa N, Suda T. A new member of tumor necrosis factor ligand family, ODF/OPGL/TRANCE/RANKL, regulates osteoclast differentiation and function. Biochem Biophys Res Commun 1999;256:449–55.

[6] Yasuda H, Shima N, Nakagawa N, Yamaguchi K, Kinosaki M, Goto M, et al. A novel molecular mechanism modulating osteoclast differentiation and function. Bone 1999;25:109–13.

[7] Yasuda H, Shima N, Nakagawa N, Yamaguchi K, Kinosaki M, Mochizuki S, et al. Osteoclast differentiation factor is a ligand for osteoprotegerin/osteoclastogenesis-inhibitory factor and is identical to TRANCE/RANKL. Proc Natl Acad Sci U S A 1998;95:3597–602.

[8] Chambers TJ. Regulation of the differentiation and function of osteoclasts. J Pathol 2000;192:4–13.

[9] Hofbauer LC, Khosla S, Dunstan CR, Lacey DL, Boyle WJ, Riggs BL. The roles of osteoprotegerin and osteoprotegerin ligand in the paracrine regulation of bone resorption. J Bone Miner Res 2000;15:2–12.

[10] Boyle WJ, Simonet WS, Lacey DL. Osteoclast differentiation and activation. Nature 2003;423:337–42.

[11] Teitelbaum SL, Ross FP. Genetic regulation of osteoclast development and function. Nat Rev Genet 2003;4:638–49.

[12] Schoppet M, Preissner KT, Hofbauer LC. RANK ligand and osteoprotegerin: paracrine regulators of bone metabolism and vascular function. Arterioscler Thromb Vasc Biol 2002;22:549–53.

[13] Kobayashi K, Takahashi N, Jimi E, Udagawa N, Takami M, Kotake S, et al. Tumor necrosis factor alpha stimulates osteoclast differentiation by a mechanism independent of the ODF/RANKL–RANK interaction. J Exp Med 2000;191:275–86.

[14] Woo KM, Choi Y, Ko SH, Ko JS, Oh KO, Kim KK. Osteoprotegerin is present on the membrane of osteoclasts isolated from mouse long bones. Exp Mol Med 2002;34:347–52.

[15] Takahashi N, Akatsu T, Udagawa N, Sasaki T, Yamaguchi A, Moseley JM, et al. Osteoblastic cells are involved in osteoclast formation. Endocrinology 1988;123:2600–2.

[16] Simonet WS, Lacey DL, Dunstan CR, Kelley M, Chang MS, Luthy R, et al. Osteoprotegerin: a novel secreted protein involved in the regulation of bone density. Cell 1997;89:309–19.
[17] Azuma Y, Kaji K, Katogi R, Takeshita S, Kudo A. Tumor necrosis factor-alpha induces differentiation of and bone resorption by osteoclasts. J Biol Chem 2000;275:4858–64.
[18] Kudo O, Fujikawa Y, Itonaga I, Sabokbar A, Torisu T, Athanasou NA. Pro-inflammatory cytokine (TNF-α/IL-1α)-induction of human osteoclast formation. J Pathol 2002;198:220–7.
[19] Kudo O, Sabokbar A, Pocock A, Itonaga I, Fujiwara Y, Athanasou NA. Interleukin-6 and interleukin-11 support human osteoclast formation by a RANKL-independent mechanism. Bone 2003;32:1–7.
[20] Wang FS, Wang CJ, Chen YJ, Huang YT, Huang HC, Chang PR, et al. Nitric oxide donor increases osteoprotegerin production and osteoclastogenesis inhibitory activity in bone marrow stromal cells from ovariectomized rats. Endocrinology 2004;145:2148–56.
[21] Arai F, Miyamoto T, Ohneda O, Inada T, Sudo T, Brasel K, et al. Commitment and differentiation of osteoclast precursor cells by the sequential expression of c-Fms and receptor activator of nuclear factor κB (RANK) receptors. J Exp Med 1999;190:1741–54.
[22] Cappellen D, Luong-Nguyen NH, Bongiovanni S, Grenet O, Wanke C, Susa M. Transcriptional program of mouse osteoclast differentiation governed by the macrophage colony-stimulating factor and the ligand for the receptor activator of NFκB. J Biol Chem 2002;277:21971–82.
[23] Takeshita S, Arai S, Kudo A. Identification and characterization of mouse bone marrow stromal cell lines immortalized by temperature-sensitive SV40 T antigen: supportive activity for osteoclast differentiation. Bone 2001;29:236–41.

ELSEVIER

Bone 37 (2005) 220 – 226

BONE

www.elsevier.com/locate/bone

Establishment of cementoblast cell lines from rat cementum lining cells by transfection with temperature-sensitive simian virus-40 T-antigen gene☆

Masae Kitagawa[a], Shoji Kitagawa[a], Yasusei Kudo[a], Ikuko Ogawa[c], Mutsumi Miyauchi[a], Hidetoshi Tahara[b], Toshinori Ide[b], Takashi Takata[a,c,*]

[a]*Department of Oral Maxillofacial Pathobiology, Division of Frontier Medical Science, Graduate School of Biomedical Sciences, Hiroshima University, 1-2-3 Kasumi, Minami-ku, Hiroshima 734-8553, Japan*

[b]*Department of Cell and Molecular Biology, Graduate School of Biomedical Sciences, Hiroshima University, Hiroshima 734-8553, Japan*

[c]*Center of Oral Clinical Examination, Hiroshima University Hospital, Hiroshima 734-8553, Japan*

Received 4 February 2005; revised 23 March 2005; accepted 5 April 2005
Available online 28 June 2005

Abstract

Defining the regulatory mechanisms promoting differentiation and proliferation of cementoblasts has not been well understood, because of the lack of cell models in vitro. To establish an in vitro cell model for the cementoblasts, extracted rat molars obtained from 8-week-old rats were used. Cells lining the root surface (cemetoblasts) were obtained by an enzymatic digestion method, and immediately immortalized by transfection of thermolabile SV40 T-antigen gene. The transfected cementum lining cell clones, RCM-C3 and -C4, were maintained for more than 200 population doublings (PD), while the original cells stopped their growth at 60 PD. Thus, immortalized cell lines decreased expression of SV40 T-antigen and subsequently cell proliferation at non-permissive temperature (39°C). Reverse-transcribed-polymerase chain reaction indicated expression of gene for type I collagen, alkaline phosphatase (ALP), osteopontin, and osteocalcin mRNA at both permissive (33°C) and non-permissive (39°C) temperatures. RCM-C4 expressed higher bone siaploprotein (BSP) mRNA than RCM-C3, and further RCM-C4 showed higher BSP mRNA at 39°C than 33°C. High ALP activity and mineralized nodule formation were observed at 39°C in both cell lines.

These findings suggested that the cell lines, RCM-C3 and -C4, are useful model for studying the regulatory mechanisms of differentiation and proliferation of cementoblasts.

Keywords: Cementoblast; Periodontal ligament; Immortalization; Transfection; SV40 T-antigen

Introduction

Cementum, a mineralized tissue produced by cementoblasts, covers the roots of teeth and provides for the attachment of periodontal ligament (PDL) to roots and surrounding alveolar bone [1]. There is general consensus that formation of cementum is essential for a new connective tissue attachment, subsequent to surgical treatment of periodontal disease [2–4]. However, research efforts toward understanding the regulatory mechanisms of the proliferation and differentiation of cells within the local region have been hampered by an inability to isolate and culture cementoblasts.

Recently, an immortalized cementoblast cell population from immortalized cementoblasts (OCCM), obtained from OC-TAg (OC = osteocalcin) transgenic mice has been established [5]. Although the cell line is a useful cell model for the study of cementoblast, transfected TAg may alter the cell nature of cementoblast.

In the present study, we used the plasmid pSV*ts*A58neo, encoding a thermolabile SV40 T-antigen (*ts*A58) to control effects of SV40 T-antigen [6–10], which inactivates the p53

☆ Grant support: This work was supported in part by Grants-in-Aid from the Ministry of Education, Science, and Culture of Japan.

* Corresponding author. Department of Oral Maxillofacial Pathobiology, Division of Frontier Medical Science, Graduate School of Biomedical Sciences, Hiroshima University, 1-2-3 Kasumi, Minami-ku, Hiroshima 734-8553, Japan. Fax: +81 82 257 5619.

E-mail address: ttakata@hiroshima-u.ac.jp (T. Takata).

8756-3282/$ - see front matter © 2005 Elsevier Inc. All rights reserved.
doi:10.1016/j.bone.2005.04.014

and Rb proteins [11–13]. Expression of SV40 T-antigen can be controlled by temperature, SV40 T-antigen being active at permissive temperature at 33°C and inactive non-permissive temperature at 39°C.

We previously reported a useful method to obtain a subpopulation enriched with cementoblasts from rat periodontal ligament by enzymatic digestion (*J. Dent. Res.* 2002;81:359). In the present study, to establish rat cementoblast cell lines, we transfected with temperature-sensitive SV40 T-antigen into cells of the subpopulation enriched with cementoblasts. We obtained two cell lines with characteristics of the cementoblasts, including high ALP activity, mineralized nodule formation, and expressions of mineralization-associated markers.

Materials and methods

These studies were performed in compliance with regulations administered by the experimentation committee of the Graduate School of Biomedical Sciences, Hiroshima University.

Isolation of the cementoblast-enriched cell population

According to our previously established method, we collected a subpopulation enriched with cells lining the root surface (cementoblasts) from rat PDL (*J. Dent. Res.* 2002;81:359). After sacrificing by an overdose of chloroform, molars were extracted from 10 Lewis male rats (8 weeks old, 220–250 g). To avoid contamination of experimental materials with gingival tissues, supracrestal soft tissues attached to the cervical area of the molars were carefully curettaged before extraction. The extracted molars with PDL were rinsed once in Dulbecco's phosphate-buffered saline (PBS) without calcium and magnesium (Nissui Pharmaceutical Co. Ltd., Tokyo, Japan). Next, they were immersed in a digestion solution, 20 ml of Dulbecco's Modified Eagle's Medium (DMEM, Nissui Pharmaceutical Co. Ltd.) containing 2 mg/ml collagenase (Wako, Tokyo, Japan) and 0.25% trypsin (Difco Laboratories, Detroit, MI, USA) at 37°C for 30 min. Tissues were exposed to digestion solution in 4 cycles for 20 min each and solutions were centrifuged to collect released PDL cells. We obtained 5 PDL-subpopulations (SP) by digestion of 30, 50, 70, 90, and 110 min. Using scanning electron microscopy, we have already confirmed that a few cells observed on the root surface after 90-min digestion were completely disappeared from the root surface after 110-min digestion. In addition, PDL-SP cells by 110-min digestion showed the highest activity of ALP and the largest number of mineralization nodules. Therefore, we are sure that PDL-SP by 110-min digestion is a subpopulation enriched with cells lining the root surface (cementoblasts) (data not shown).

In this study, we used the PDL-SP cells by 110-min digestion which were interpreted as a subpopulation enriched with cementoblasts. The cells were cultured in DMEM with 10% fetal bovine serum (FBS) plus penicillin G solution (10 units/ml) and streptomycin (10 mg/ml) in a humidified atmosphere of 5% CO_2 at 37°C.

Transfection with a thermolabile SV40 T-antigen gene

The pSV*ts*A58neo was kindly provided by M. Obitana (Department of Cell Biology, Institute of Development, Aging and Cancer, Tohoku University). We seeded 1×10^6 cells in 90-mm culture dishes 1 day before transfection and incubated the cells at 37°C until cells were 60%–80% confluent. Transfection was performed at 33°C with Lipofectamine Plus (Life Technologies Inc., Grand Island, NY), according to the manufacturer's protocol. Clones grown in the presence of 400 μg/ml G418 were ring-cloned, expanded, and tested for the presence of T-antigen. Cell clones were maintained in 90-mm culture dishes containing 6 ml of medium at 33°C and subcultivated at a split ratio permitting cells to be subcultured approximately once per 4 days. The split ratio varied according to the clone population doublings (PD) from 1:2 to 1:8.

Cell growth assay to assess the effect of cultural temperature

5000 cells were plated in 24-well multiwell plate with incubation for 24 h. The culture medium was then replaced with fresh medium and cells were cultured at 33°C or 39°C. Trypsinized cells were counted using a cell counter (Coulter Z1, Coulter Corp, Hialeah, Florida) at 0, 3, and 5 days.

Determination of SV40 T-antigen expression by Western blot analysis

Subconfluent cells, in 90-mm culture dishes, were used for Western blot analysis. Cells were lysed in Mammalian Protein Extraction Reagent (M-PER™; PIERCE, Rockford, IL). Protein concentration was determined by Bradford protein assay (BioRad, Laboratories, Richmond, CA) using bovine serum albumin (Sigma Chemical Co., St. Louis, MO) as a standard. 50 μg/ml of protein was solubilized in Laemmli sample buffer by boiling, and subjected to 7.5% sodium dodecylsulfate-polyacrylamide gel electrophoresis (SDS-PAGE), followed by electroblotting onto a PVDF filter treated with methanol. The filter was blocked for 1 h at 4°C with phosphate-buffered saline (PBS) buffer (137 mM NaCl, 8.1 mM $Na_2HPO_412H_2O$, 2.68 mM KCl, 1.47 mM KH_2PO_4) containing 5% nonfat dry milk powder. Western blot analysis was performed using an anti-SV40 T-antigen monoclonal antibody (Pab 101, Santa Cruz Biotechnology, Santa Cruz, CA) dissolved in PBS containing 5% nonfat dry milk powder and incubating for 60 min at room temperature. Incubation with a secondary peroxidase-coupled goat anti-mouse antibody was performed under the same conditions. For detection of the immunocomplex, an ECL

Western blotting detection system (Amersham Pharmacia Biotech., Tokyo, Japan) was used.

Measurement of ALP activity

ALP activity was assayed histochemically and biochemically. Cells were plated in 24-well multiwell plates (5×10^4 cells per well) and cultured in DMEM containing 10% FBS, penicillin G sodium (10 units/ml) and streptomycin sulfate (10 mg/ml) for 3, 6, and 9 days after confluent. Histochemical staining was performed according to a modified new fuchsin method. Briefly, after the rinse with 0.05 M Tris–HCl (pH 7.4) for 5 min at room temperature, the cells were stained with 0.05 M Tris–HCl (pH 9.8) containing 10 mg/ml of sodium naphthol AS-BI phosphate salt (Sigma-Aldrich Co., MO), 4% new fuchsin solution, and 4% sodium nitrite for 30 min. Then, the cells were fixed with 10% formaldehyde neutral buffer solution (Katayama Chemical, Tokyo, Japan) for 60 min and ALP activity was histochemically observed by light microscopy.

The quantitative analysis of ALP activity was performed biochemically by Bessey–Lowry enzymologic method using nitrophenyl phosphate as a substrate [14]. Cells were plated in 24-well multiwell plates (5×10^4 cells per well, $n = 4$) and cultured in DMEM containing 10% FBS, penicillin G sodium (10 units/ml) and streptomycin sulfate (10 mg/ml) for 5 days after confluent. The cells were washed with PBS and homogenized ultrasonically in 0.5 ml of 10 mM Tris–HCl buffer (pH 7.4) containing 25 mM $MgCl_2$. Aliquots of the homogenates were used for quantification of ALP activity.

Mineralization assay

Mineral nodule formation was detected by alizarin red S (ALZ) staining for calcium [15]. Cells were placed in a 24-well multiwell plate at a density of 5×10^4 cells per well and cultured in DMEM supplemented with 10% FBS, 50 mg/ml ascorbic acid, 10 mM sodium β-glycerophosphate, and 10 nM dexamethsone at 39°C for 3, 6, and 9 days after confluent. The cells were fixed in a 3.5% formaldehyde neutral buffer solution, and then stained with ALZ.

RNA preparation and reverse transcription-polymerase chain reaction analysis (RT-PCR)

Total RNA was isolated from cultures of confluent cells at 33°C or 39°C using the RNeasy Mini Kit (Qiagen K.K., Tokyo, Japan) according to the manufacturer's instructions. Preparations were quantified and their purity was determined by standard spectrophometric methods. cDNA was synthesized from 1 μg of total RNA according to the ReverTra Dash (Toyobo Biochemicals, Tokyo, Japan). The oligonucleotide RT-PCR primers for type I collagen (COLI), ALP, osteopontin (OPN), osteocalcin (OCN), bone sialoprotein (BSP), and glyceraldehydes-3-phosohate (GAPDH) listed in Table 1 were purchased from Invitrogen (Tokyo, Japan). Aliquots of total cDNA were amplified with 1.25 U of rTaq-DNA polymerase (Qiagen K.K.), and amplifications were performed in a PC701 thermal cycler (Astec, Fukuoka, Japan) for 30 (COLI, ALP, OPN, and OCN) and 35 (BSP) cycles after an initial 30 s denaturation at 94°C, annealed for 30 s at 56°C, and extended for 1 min at 72°C in all primers. The amplification reaction products were resolved on 1.5% agarose/TAE gels (Katayama Chemical), electrophoresed at 100 mV, and visualized by ethidium-bromide staining.

Transplantation

We transplanted cells into immunodeficient mouse. 1×10^7 cells in 100 μl of PBS were inoculated subcutaneously into 4-week-old male BALB/cAnNcrj-nu mice (Charles River Japan, Inc., Kanagawa, Japan, $n = 3$). After 3 months, we observed the transplants.

Statistical analysis

The results of cell growth analysis and quantitative ALP activity were shown as mean ± SE. According to Fisher's system, the mean values were analyzed for significance using Wilcoxon's test for non-paired examination. P values of less than 0.05 or 0.01 were judged to be statistically significant.

Results

Establishment of rat cementoblast (RCM) cell lines

Four clones (RCM-C1, -C2, -C3, -C4) were obtained by transfection with the pSV*ts*A58neo. These clones could be subcultured over 200 PD (Fig. 1A), while non-transfected original cells stopped their growth about 60 PD. We used two clones (RCM-C3 and -C4) in the following studies, because the clones showed high activities of ALP and mineralization in vitro. These cell clones showed polygonal

Table 1
Oligonucleotide primer sequences utilized in the RT-PCR

RT-PCR primer set	Sequence	Product length (bp)
COLI	F 5′-ctgaccttcctgcgcctgatgtcc-3′ R 5′-gtctggggcaccaacgtccaaggg-3′	300
ALP	F 5′-aggcaggattgaccacgg-3′ R 5-tgtagttctgctcatgga-3	440
OPN	F 5′-tccaaggagtataagcagcgggcca-3′ R 5′-ctcttagggtctaggactagcttct-3′	200
OCN	F 5′-cagcccctacccagat-3′ R 5′-gaaagtatggacggcaca-3′	232
BSP	F 5′-cactcacttgctctctccag-3′ R 5-ctgagagtgtggcgttgtgt-3	385
GAPDH	F 5′-tccaccaccctgttgctgta-3′ R 5′-accacagtccatgccatcac-3′	450

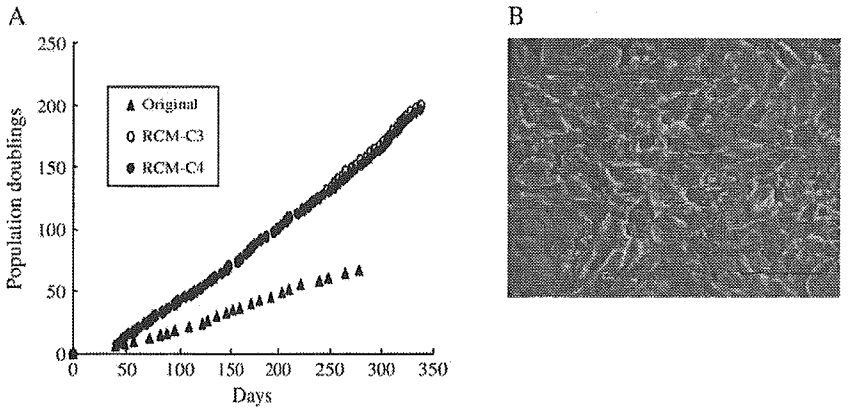

Fig. 1. (A) Population doublings (PD) of RCM cells. Original cells (Origin) stopped about 60 PD, but SV40 T-antigen-transfected clones (RCM-C3 and -C4) are immortalized and grow over 200 PD. (B) The morphology of RCM cells in culture. RCM cells were polygonal morphology and grew in monolayer (scale bar = 100 μm).

morphology in shape similar to original cells, and grew in monolayer at 39°C (Fig. 1B).

Cell proliferation of RCM cells at the permissive (33°C) or non-permissive temperatures (39°C)

Growth of the cells was significantly inhibited under the non-permissive condition, 39°C (Fig. 2A). The expression of T-antigen was decreased at 39°C compared with 33°C in both RCM cell lines (Fig. 2B).

Characterization of RCM cells

Expression of COLI, ALP, OPN, and OCN mRNA were observed in RCM-C3 and -C4 at both 33°C and 39°C (Fig. 3A). RCM-C4 expressed higher levels of BSP mRNA than RCM-C3, with greater BSP mRNA levels at 39°C vs. 33°C (Fig. 3A). Both cell lines showed higher ALP activity at 39°C than at 33°C on the 5th day (Fig. 3B). By histochemical method, both RCM-C3 and -C4 showed intense staining of ALP on the 6th day, but weak staining on the 3rd and 9th day (Figs. 3C a–c, g–i) at 39°C. RCM-C3 showed intense ALZ staining on the 6th and 9th day (Figs. 3C d–f), and RCM-C4 showed slight staining on the 6th day, and increased intensity on the 9th day (Figs. 3C j–l) at 39°C. No positive staining of ALP and ALZ was detected at 33°C in both cell lines (data not shown). Positive staining of ALZ was not observed in cells cultured in medium without supplements (50 μg/ml ascorbic acid, 10 mM β-glycerophosphate and 10 nM dexamethasone) even at 39°C (data not shown).

Transplantation of RCM cells

After 3 months, RCM cell lines transfected with SV40 T-antigen had no tumorigenesis (data not shown).

Discussion

Several efforts have been made to define the mechanism, controlling the differentiation and proliferation of cementoblasts [16–24]. However, detailed regulatory mechanisms have not yet to be completely elucidated. One of the factors hindering the detailed analyses is the lack of a stable in vitro cell model for cementoblasts.

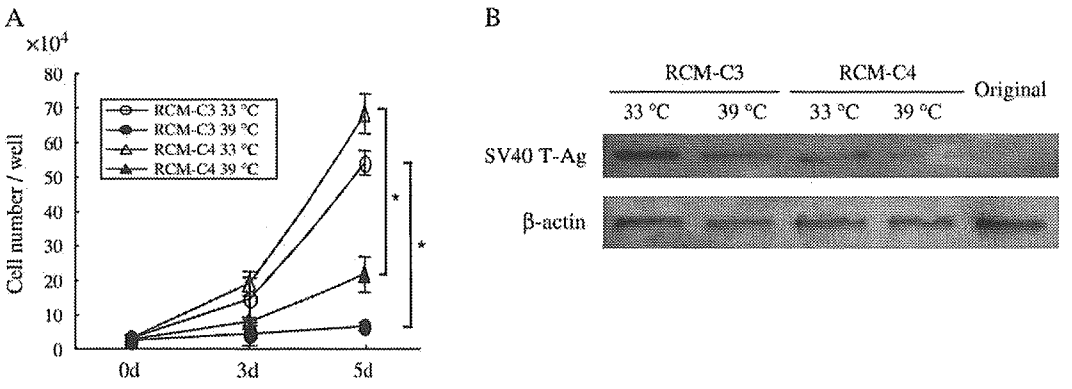

Fig. 2. (A) Growth of RCM-C3 and -C4 cells at 33°C and 39°C. *Significant difference ($P < 0.01$). (B) Expression of SV40 T-antigen in RCM-C3 and -C4 cells at 33°C and 39°C. In both cell lines, the amount of T-antigen is decreased at 39°C compared to 33°C.

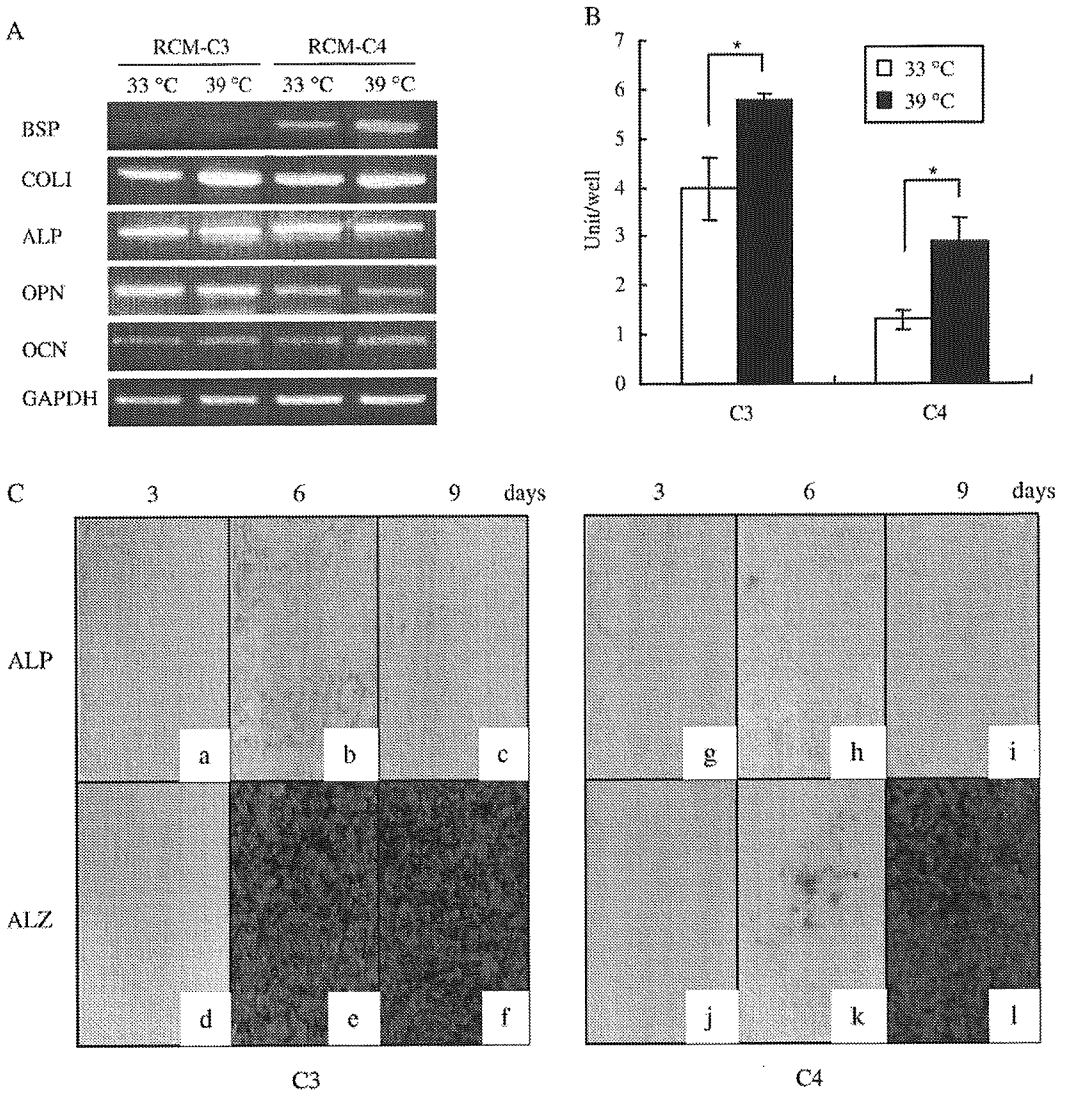

Fig. 3. (A) Gene expression of COLI, ALP, OPN, OCN, and BSP by RT-PCR in RCM-C3 and -C4 at 33°C and 39°C. (B) ALP activity by biochemical method. RCM-C3 and -C4 cells were cultured for 5 days after confluent. Both cell lines showed higher ALP activity at 39°C than 33°C. *Significant difference ($P < 0.05$). (C) ALP activity by histochemical method (a, b, c, g, h, i) and mineralization (d, e, f, j, k, l). RCM-C3 (a–f) and C4 (g–l) cells were cultured in DMEM containing 10% FBS with supplements for 3 (a, d, g, j), 6 (b, e, h, k), and 9 (c, f, i, l) days at 39°C.

In the present study, we established immortalized cementoblast cell lines, RCM-C3 and RCM-C4, by transfection with the thermolabile SV40 T-antigen into root lining cell subpopulations obtained from adult rat molars. SV40 T-antigen, which inactivates the p53 and Rb proteins, has been used to immortalize rodent and human cells [25–30]. Transfection with SV40 T-antigen results in an expanded life span for cells. The cell lines established here have continued to proliferate more 200 PD at 33°C and have not undergone senescence. The advantage of thermolabile SV40 T-antigen is to minimize the effects of transforming oncogene at the non-permissive temperature. The expression of SV40 T-antigen by RCM-C3 and -C4 disappeared at 39°C, and proliferative activity of RCM-C3 and -C4 markedly decreased. These results demonstrate that transfection of thermolabile SV40 T-antigen is effective in immortalized cells but also provide a means to examine cells under minimal effects of the antigen. Therefore, the cell line established in this study showed less effect of transformable changes, in comparison with cell lines transfected with non-thermolabile SV40 T-antigen. In addition, the shift of temperature from permissive temperature (33°C) to non-permissive temperature (39°C) induced the inhibition of proliferation and promotion of differentiation.

Cultured RCM-C3 and -C4 cells displayed the same polygonal morphology as the parent cells and grew in monolayer. Furthermore, we confirmed that RCM cell lines transfected with SV40 T-antigen had no tumorigenesis by transplantation (data not shown). This finding is consistent with the previous reports that most SV40 large T-immortalized cell lines preserve contact inhibition [31–33].

Cells immortalized with thermolabile SV40 T-antigen proliferate under permissive temperature (33°C), whereas they differentiate at non-permissive temperature (39°C). ALP activity increased at 39°C in RCM-C3 and -C4 cells. Consistent with this, RCM-C4 exhibited higher BSP mRNA levels, one of the mineralization-associated markers [34], at 39°C than 33°C.

These two cell lines expressed other mineralization-associated markers [34,35], such as COLI, ALP, OPN, and OCN mRNA, at both 33°C and 39°C by RT-PCR. These genes, shown by RT-PCR, are similar to genes reported by others to be associated with cementoblast phenotype. MacNeil et al. demonstrated that OPN, OCN, and BSP, major components of cementum, are secreted by root lining cells, cementoblasts, using immunocytochemical and in situ hybridization [36–38]. According to their study, BSP and OCN are expressed selectively in the cells lining root surface (cementoblasts) and are not expressed in PDL cells at any stage of development. In contrast, some reports that PDL cells are references to a small group of "STEM CELLS" do express OCN/BSP [39]. Nevertheless, we considered RCM-C3 and -C4 cementoblasts based on high expression of BSP or OCN as well as intense staining of ALP and ALZ by histochemical analyses. Histological staining demonstrated that the high ALP activity observed at day 6 was markedly reduced at day 9 and intense ALZ staining, suggestive of high mineralization, was observed. In support of the finding, Stain et al. reported that as osteoblast cells progress toward the mineralization stage, they exhibit measured ALP activity, histochemically, and increase mineral nodular formation, but levels of ALP mRNA decline [35].

Overall, these findings suggest that RCM-C3 and -C4 cell lines will be useful for determining mechanisms that regulate the differentiation and proliferation of cementoblasts. To examine that cell lines continue to keep the ability to produce mineral in vivo, we will try to transplant RCM cell lines in nude mice with hydroxyapatipte beads as the attachment material of cells in the future.

Acknowledgment

We are grateful to Dr. Somerman MJ for the advice and discussions during the course of this work.

References

[1] Ten Cate AR. The periodontium: oral histology: development, structure and function. Mosby: St. Louis; 2003. p. 276–9.
[2] Ten Cate AR, Mills C, Solomon G. The development of the periodontium. A transplantation and autoradiographic study. Anat Rec 1971;170:365–79.
[3] Ten Cate AR, Mills C. The development of the periodontium: the origin of alveolar bone. Anat Rec 1972;173:69–77.
[4] Ten Cate AR. Development of the periodontium. In: Cate Ten, editor. Oral histology, 4th ed. Mosby: St. Louis; 1994. p. 257–75.
[5] D'Errico JA, Ouyang H, Berry JE, MacNeil RL, Strayhorn C, Imperiale MJ, et al. Immortalized cementoblasts and periodontal ligament cells in culture. Bone 1999;25:39–47.
[6] Ide T, Tsuji Y, Nakashima T, Ishibashi S. Progress of aging in human diploid cells transformed with a tsA mutant of simirian virus 40. Exp Cell Res 1984;150:321–8.
[7] Jat PS, Noble MD, Ataliotis P, Tanaka Y, Yannoutsos N, Larsen L, et al. Direct derivation of conditionally immortal cell lines from an H-2Kb-ts58 transgenic mouse. Proc Natl Acad Sci U S A 1991;88: 5096–5100.
[8] Manfredi JJ, Prives C. The transforming activity of simian virus 40 large tumor antigen. Biochim Biophys Acta 1994;1198: 65–83.
[9] Tegtmeyer P. Function of simian virus 40 gene A in transforming infection. J Virol 1975;15:612–8.
[10] Yanai N, Suzuki M, Obitana M. Hepatocyte cell lines established from transgenic mice harboring temperature-sensitive simirian virus 40 large T-antigen gene. Exp Cell Res 1991;197:50–6.
[11] Eliyahu D, Raz A, Gruss P, Givol D, Oren M. Participation of p53 cellular tumour antigen in transformation of normal embryonic cells. Nature 1984;312:646–9.
[12] Jenkins JR, Rudge K, Currie GA. Cellular immortalization by a cDNA clone encoding the transformation-associated phosphoprotein p53. Nature 1984;312:651–4.
[13] Rassoulzadegan M, Cowie A, Carr A, Glaichenhaus N, Kamen R, Cuzin F. The roles of individual polyoma virus early proteins in oncogenic transformation. Nature 1982;300:713–8.
[14] Bessey OA, Lowry OH, Brock MJ. A method for the rapid detemination of alkaline phosphatase with five cubic millimeter of serum. J Biol Chem 1946;164:321–9.
[15] Dahl LK. A simple and sensitive histochemical method for calcium. Proc Soc Exp Biol Med 1952;80:474–9.
[16] Bosshardt DD, Zalzal S, McKee MD, Nanci A. A developmental appearance and ditribution of bone sialoprotein and osteopontin in human and rat cementum. Anat Rec 1998;250:13–33.
[17] D'Errico JA, Berry JE, Ouyang H, Strayhorn C, Windle JJ, Somerman MJ. Employing a transgenic animal model to obtain cementoblasts, in vitro. J Periodontol 2000;71:63–72.
[18] Grzesik WJ, Kuznetsov SA, Uzawa K, Mankani M, Gehron Robey P, Yamauchi M. Normal human cementum-derived cells: isolation, clonal expansion, and in vitro and in vivo characterization. J Bone Miner Res 1998;13:547–1554.
[19] MacNeil RL, D'Errico JA, Ouyang H, Berry J, Strayhorn C, Somerman MJ. Isolation of murine cementoblasts: unique cells or uniquely-positioned osteoblasts? Eur J Oral Sci 1998;106(Suppl I): 350–6.
[20] Nohutcu RM, McCauley LK, Koh AJ, Somerman MJ. Expression of extracellular matrix proteins in human periodontal ligament cells during mineralization in vitro. J Periodontol 1997;68:320–7.
[21] Ouyang H, McCauley LK, Berry JE, D'Errico JA, Strayhorn CL, Somerman MJ. Response of immortalized murine cementoblasts/periodontal ligament cells to parathyroid hormone and parathyroid hormone-related protein in vitro. Arch Oral Biol 2000;45: 293–303.
[22] Ouyang H, McCauley LK, Berry JE, Saygin NE, Tokiyasu Y, Somerman MJ. Parathyroid hormone-related protein regulates extracellular matrix gene expression in cementoblasts and inhibits cementoblast-mediated mineralization in vitro. J Bone Miner Res 2000;15:2140–2153.
[23] Ramakrishnan PR, Lin WL, Sodek J, Cho MI. Synthesis of non-collagenous extracellular matrix proteins during development of mineralized nodules by rat periodontal ligament cells in vitro. Calcif Tissue Int 1995;57:52–9.
[24] Saygin N, Giannobile WV, Somerman MJ. Molecular and cell biology of cementum. Periodontology 2000;24:73–98.

[25] Jat PS, Sharp PA. Large T antigens of simian virus 40 and polyomavirus efficiently establish primary fibroblasts. J Virol 1986;59:746–50.
[26] Petit CA, Gardes M, Feunteun J. Immortalization of rodent embryo fibroblasts by SV40 is maintained by the A gene. Virology 1983;127: 74–82.
[27] Powell AJ, Darmon AJ, Gonos ES, Lam EW, Peden KW, Jat PS. Different functions are required for initiation and maintenance of immortalization of rat embryo fibroblasts by SV40 large T antigen. Oncogene 1999;18:7343–50.
[28] Shay JW, Van Der Haegen BA, Ying Y, Wright WE. The frequency of immortalization of human fibroblasts and mammary epithelial cells transfected with SV40 large T-antigen. Exp Cell Res 1993;209:45–52.
[29] Todaro GJ, Green H. Quantitative studies of the growth of mouse embryo cells in culture and their development into established lines. J Cell Biol 1963;17:299–313.
[30] Yanai N, Satoh T, Kyo S, Abe K, Suzuki M, Obitana M. A tubule cell line established from transgenic mice harboring temperature-sensitive simirian virus 40 large T-antigen gene. Jpn J Cancer Res 1991;82: 1344–1348.
[31] Meek RL, Bowman PD, Daniel CW. Establishment of mouse embryo cells in vitro. Relationship of DNA synthesis, senescence and malignant transformation. Exp Cell Res 1977;107:277–84.
[32] Wieser RJ, Faust D, Dietrich C, Oesch F. p16INL4a mediates contact inhibition of growth. Oncogene 1999;18:228–77.
[33] Zhang HS, Postigo AA, Dean DC. Active transcriptional repression by the Rb-E2F complex mediates G1 arrest triggered by p16INK4a, TGF-β, and contact inhibition. Cell 1999;97:53–61.
[34] Aubin JE, Liu F, Malaval L, Gupta AK. Osteoblast and chondroblast differentiation. Bone 1995;17:77S–83S [Suppl].
[35] Stain GS, Lian JB. Molecular mechanisms mediation proliferation/ differentiation interrelationships during progressive development of osteoblast phenotype. Endocr Rev 1993;14:424–42.
[36] D'Errico JA, MacNeil RL, Takata T, Berry J, Strayhorn C, Somerman MJ. Expression of bone associated markers by tooth root lining cells, in situ and in vitro. Bone 1997;20:117–26.
[37] MacNeil RL, Sheng N, Strayhorn C, Fishier LW, Somerman MJ. Bone sialoprotein is localized to the root surface during cementogenesis. J Bone Miner Res 1994;9:1597–606.
[38] Macneil RL, Berry J, Strayhorn C, Somerman MJ. Expression of bone sialoprotein mRNA by cells lining the mouse tooth root during cementogenesis. Arch Oral Biol 1996;41:827–35.
[39] Berry JE, Zhao M, Jin Q, Foster BL, Viswanathan H, Somerman MJ. Exploring the origin of cementoblasts and trigger factors. Connect Tissue Res 2003;44:97–102.

ELSEVIER

Bone 38 (2006) 420–426

BONE

www.elsevier.com/locate/bone

Characteristics of periodontal ligament subpopulations obtained by sequential enzymatic digestion of rat molar periodontal ligament

T. Kaneda [a,b], M. Miyauchi [a], T. Takekoshi [a], S. Kitagawa [a], M. Kitagawa [a], H. Shiba [b], H. Kurihara [b], T. Takata [a,*]

[a] *Department of Oral Maxillofacial Pathobiology, Division of Frontier Medical Science, Graduate School of Biomedical Sciences, Hiroshima University, 1-2-3 Kasumi, Minami-ku, Hiroshima 734-8553, Japan*

[b] *Department of Periodontal Medicine, Division of Frontier Medical Science, Graduate School of Biomedical Sciences, Hiroshima University, 1-2-3 Kasumi, Minami-ku, Hiroshima 734-8553, Japan*

Received 6 December 2004; revised 13 July 2005; accepted 17 August 2005
Available online 20 October 2005

Abstract

Periodontal ligament (PDL) consists of different cell populations in various differentiation stages. In the present study, we isolated cell populations from rat molar PDL by sequential enzymatic digestion and characterized growth potential and mineralization activity of the PDL subpopulations (PDL-SP) to throw light on the mechanism of PDL remodeling and, in its turn, periodontal tissue regeneration. PDL attached to extracted rat molars was digested 2 mg/ml collagenase and 0.25% trypsin at 37°C for 30 min. Then four consecutive digestions were performed for 20 min each in a fresh digestive solution. The solutions were centrifuged to collect released cells and 5 PDL subpopulations (30M-, 50M-, 70M-, 90M-and 110M-PDL-SP) were obtained. Light microscopic observation showed that about a half of PDL in width attached on the root surface of extracted teeth and 30M-PDL-SP was considered to contain cells mainly from middle portion of PDL. Scanning electron microscopic examination indicated that 110M-PDL-SP was enriched by root lining cementoblastic cells. 30M-PDL-SP showed a high level of proliferative activity. Although the growth potential of a subpopulation decreased in PDL-SP toward the root surface, 110M-PDL-SP had a high proliferative activity equivalent to that of 30M-PDL-SP. Analyses of alkaline phosphatase (ALP) and mineralization activities showed that higher activities in PDL-SP toward the surface of roots and that 110M-PDL-SP had the highest activity of ALP and the largest number of mineralization nodules. The present study shows as supposed by previous studies on cell kinetics in PDL that subpopulations with larger growth potential were generally located in the middle portion of PDL and those with higher mineralization activities toward the surface of the roots. It is suggested, however, that a possible pathway of PDL cell turnover may exist within the PDL-SP on the root surface in addition to the generally recognized pathway from the middle area of PDL to root surface.

Keywords: Periodontal ligament; Proliferation; Mineralization; Sequential enzymatic digestion

Introduction

Periodontal ligament (PDL), a thin connective tissue between root cementum and alveolar bone, plays important roles such as supportive, sensory, nutritive and homeostatic functions [1,2]. Recent studies showed, furthermore, that the formative function of PDL is indispensable to consider regenerative periodontal therapies [1,2].

It has been reported that PDL cells have osteoblastic characters, such as expressing high activity of alkaline phosphatase (ALP) [3,4], synthesizing cAMP at the stimulation of parathyroid hormone [5], producing mineralized nodules in vitro in the presence of ascorbic acid (50 μg/ml), dexanethasone (5 μM) and β-glycerophosphate (10 mM) [6], and producing non-collagenous proteins such as osteopontin (OPN), osteocalcin (OCN), and bone sialoprotein (BSP) [6,7]. In these studies, however, PDL was examined as a tissue unit and PDL-derived cells were characterized in the lump.

* Corresponding author. Fax: +81 82 257 5619.
E-mail addresses: mmiya@hiroshima-u.ac.jp (M. Miyauchi), mhiraoka@hiroshima-u.ac.jp (M. Kitagawa), shiba@hiroshima-u.ac.jp (H. Shiba), hkuri@hiroshima-u.ac.jp (H. Kurihara), ttakata@hiroshima-u.ac.jp (T. Takata).

8756-3282/$ - see front matter © 2005 Elsevier Inc. All rights reserved.
doi:10.1016/j.bone.2005.08.021

McCulloch et al. [8,9] reported that progenitor cells in marrow spaces migrate into PDL by way of vascular channels and locate perivascularly. The progenitor cells then provide daughter cells that migrate to the bone and cementum surfaces and differentiate into cementoblasts or osteoblasts. Perivascular cells also considered to be the source of PDL fibroblasts. These findings suggest that PDL consists of different cell populations in various differentiation stages according to the position in PDL.

Sequential enzymatic digestion has been applied to obtain the different cell populations from bone tissue. Wong and Cohn obtained 6 subpopulations of bone cells by sequential digestion of mouse calvaria with collagenase and trypsin [10]. They showed that bone contains at least two types of target cells with different response to parathormone and calcitonin. Rao et al. also showed that cell populations obtained from rat calvaria by the same method had different response to parathyroid hormone or prostaglandin E1 [11]. Using enzymatic digestion, PDL cells obtained from tissues adherent to the extracted root surface in some studies and cellular characteristics of the cells were studied [12,13]. As mentioned above, however, the cells were harvested in the lump and analyzed as a tissue unit in those studies. D'Errico et al. [12] isolated a heterogeneous primary cell population of PDL cells from extracted root surface using 2-hour-enzymatic digestion, and demonstrated that root lining cells (cementoblasts) expressing OPN, OCN and BSP were included within the isolated PDL cells. So we considered that different PDL subpopulations (PDL-SPs) in various differentiation stages including PDL-SP enriched with cementoblasts located on root surface may be successfully isolated by sequential enzymatic digestion. The isolated PDL-SPs may be useful to determine regulation of the mechanisms of differentiation and proliferation of PDL and cementoblasts. Moreover they may be useful tool to establish the in vitro cell system.

In the present study, therefore, we reported the isolation of cell populations from rat molar PDL by sequential enzymatic digestion and characterized the growth potential and mineralization activity of PDL-SPs to throw light on the mechanism of remodeling of PDL.

Materials and methods

Isolation of PDL subpopulations and cell culture

The protocol of the studies was approved by the experimentation committee of the Faculty of Dentistry, Hiroshima University. After sacrificing by an overdose of chloroform, 100 molars were extracted from 10 Lewis male rats (8-week old, 220–250 g). To avoid contamination of gingival tissues, supracrestal soft tissues attached to the cervical area of the molars were carefully curretaged before the extraction. The extracted molars with PDL were rinsed once in Dulbecco's phosphate-buffered saline without calcium and magnesium (PBS, NISSUI PHARMACEUTICAL CO., LTD., Tokyo, Japan). Then, they were immersed in a digestion solution, 20 mL of Dulbecco's Modified Eagle Medium (DMEM) (Gibco BRL, N.Y, USA) containing 2 mg/mL collagenase (Wako, Tokyo, Japan) and 0.25% trypsin (DIFCO LABORATORIES, MI, USA), at 37°C for 30 min [12,13]. After that, four consecutive digestions were performed for 20 min each in a fresh solution. The solutions were centrifuged to collect released PDL cells. In this way, 5 PDL-SPs were obtained and named 30M-, 50M-, 70M-, 90M-and 110M-PDL-SP, respectively. The cells in each subpopulations were then cultured in DMEM with 10% fetal bovine serum (FBS) plus penicillin G sodium (10 unites/mL) and streptomycin sulfate (10 mg/mL) in a humidified atmosphere of 5% CO_2 at 37°C. The culture medium was changed once three days and cells at the third to fifth passages were used in following studies.

Light microscopic observation

To examine the amount of PDL attached to the root surface of extracted molars and the effect of sequential enzymatic digestion of the PDL, light microscopic observations with conventional and phase contrast microscopes were performed on some extracted teeth before and after the enzymatic digestion. For hematoxylin and eosin sections, the teeth were fixed in a 10% formaldehyde neutral buffer solution overnight, decalcified in a 10% EDTA solution (pH 7.4) for 2 weeks at 4°C and cut into paraffin embedded 4.5-micrometer section routinely.

Scanning electron microscopic observation

To observe the surface condition of digested PDL and root surface, each 3 teeth were prepared for scanning electron microscopy (SEM) at each digestion period. After gentle wash with PBS, the teeth were fixed in a 0.1 M cacodylate-buffered 2% paraformaldehyde and 2.5% glutaraldehyde solution (pH 7.4, 4°C) for 1 hour. The teeth were then post-fixed in a 0.1 M cacodylate-buffered 1% OsO4 solution (pH 7.4, 4°C) for 1 hour. They were dehydrated in a graded series of ethanol, critical-point-dried, and sputter-coated with gold-palladium. The specimens were examined in a JSM-6300 scanning electron microscope (Japan Electron Co., Tokyo) at 60 kv.

Cell growth analysis of PDL subpopulations

PDL cells of the subpopulations were plated in 24 well culture-plates at an initial density of 5×10^3 cells per well and cultured in DMEM containing 10% FBS, penicillin G sodium (10 unites/mL) and streptomycin sulfate (10 mg/mL). At day 2, 4 and 8, the cells were harvested, in triplicate wells, by incubating in 0.05% trypsin and 0.01% EDTA, and cell number were determined by Coulter counter Z1 (Coulter Electronic Ltd., UK). Morphology of the cultured PDL cells was observed by a phase-contrast microscope.

ALP-Activity of PDL subpopulations

ALP activity was assayed by biochemical methods. Cells of each PDL-SP were plated in 24 well culture plates (5×10^4 cells per well) and cultured in DMEM containing 10% FBS, penicillin G sodium (10 unites/mL) and streptomycin sulfate (10 mg/mL) for one week.

The quantitative analysis of ALP activity was performed by Bessey-Lowry enzymologic method using nitrophenyl phosphate as a substrate [14]. The cells were washed with PBS and homogenized ultrasonically in 0.5 mL of 10 mM Tris-HCl buffer (pH 7.4) containing 25 mM $MgCl_2$. Aliquots of the homogenates were used for determination of ALP activity and DNA content. One unite of ALP was defined as the amount of enzyme required to hydrolyze 1 nM *p*-nitrophenol per minute. DNA content was determined using bisbenzimidazole (Wako, Osaka, Japan) and ALP activities of PDL-SPs were expressed by unites per DNA contents.

Mineralization of PDL Cells

Mineralized nodule formation was examined by Dahl's stain for calcium [15]. Cells of PDL-SP were plated in 24 well-culture plates at a density of 5×10^4 cells per well and cultured in DMEM supplemented with 10% FBS, 50 μg/mL ascorbic acid, 10 mM sodium β-glycerophosphate and 10 nM dexamethasone for 3 weeks. Then the cells were fixed in a 10% formaldehyde neutral buffer solution and stained with alizarin red S. To clarify the nature of mineralized nodules, immunostaining for bone sialoprotein (BSP) was done. After blocking nonspecific staining with 0.5% casein for 20 min at RT, a rabbit polyclonal anti-BSP antibody (AB1854; CHEMICON, CA) was applied to 2% formaldehyde fixed cells at dilution of 1:500. Immunostaining was carried out using Dako-LSB2 kit (Dako, CA). The color developed with 0.025% 3,3′-diaminobenzidine

Table 1
Oligonucleotide primer sequences utilized in the RT-PCR

RT-PCR primer set		Sequence	Product length (bp)
COLI	F	5′-ctgaccttcctgcgcctgatgtcc-3′	300
	R	5′-gtctggggcaccaacgtccaaggg-3′	
ALP	F	5′-aggcaggattgaccacgg-3′	440
	R	5′-tgtagttctgctcatgga-3′	
OPN	F	5′-tccaaggagtataagcagcgggcca-3′	200
	R	5′-ctcttagggtctaggactagcttct-3′	
OCN	F	5′-cagccccctacccagat-3′	232
	R	5′-gaaagtatggacggcaca-3′	
BSP	F	5′-cactcacttgctctctccag-3′	385
	R	5′-ctgagagtgtggcgttgtgt-3′	
GAPDH	F	5′-tccaccaccctgttgctgta-3′	450
	R	5′-accacagtccatgccatcac-3′	

tetrahydrochloride in TRIS-HCL buffer plus hydrogenperoxide (Kyowa Medics, Tokyo). The cells were counterstained with Mayer's hematoxylin, dehydrated and then mounted.

Statistical analysis

Enumeration assay of triplicate wells was repeated 3 times. Total 9 wells were assayed in each experimental group. The results of cell growth analysis and quantitative analysis of ALP activity were shown as mean ± SE. The mean values obtained were analyzed for statistical differences using a nonparametric Mann-Whitney U-test. Probabilities less than 0.05 were considered as significant.

RNA preparation and reverse transcription-polymerase chain reaction analysis (RT-PCR)

Total RNA was isolated from cultures of confluent 30M-and 110M-PDL-SP cells using the RNeasy Mini Kit (Qiagen K.K., Tokyo, Japan) according to the manufacture's instructions. Preparations were quantified and their purity was determined by standard spectrophometric methods. cDNA was synthesized from 1 μg of total RNA according to the ReverTra Dash (Toyobo Biochemicals, Tokyo, Japan). The oligonucleotide RT-PCR primers for type I collagen (COLI), ALP, osteopontin (OPN), osteocalcin (OCN), BSP and glyceraldehydes-3-phosohate (GAPDH) listed in Table 1 were purchased from Invitrogen (Tokyo, Japan). Aliquots of total cDNA were amplified with 1.25 U of rTaq-DNA polymerase (Qiagen K.K.), and amplifications were performed in a PC701 thermal cycler (Astec, Fukuoka, Japan) for 32 cycles after an initial 30 sec denaturation at 94°C, annealed for 30 sec at 56°C, and extended for 1 min at 72°C in all primers. The amplification reaction products were resolved on 1.5% agarose/TAE gels (Katayama Chemical), electrophoresed at 100 mV, and visualized by ethidium-bromide staining.

Immunohistochemistry for BrdU incorporated and proliferating cell nuclear antigen (PCNA) in vivo rat PDL

To evaluate of cell proliferative activity in vivo PDL tissue, immunohistochemistry for BrdU and PCNA was done. Male 8-week-old Lewis rats were sacrificed by over dose of ethyl ether. At 2 hr before sacrifice, all rats ($n = 3$) were given a single intraperitoneal injection of BrdU (Sigma, St Louis) at a dosage of 100mg/kg body weight. Tissue samples were resected en block from molar region and fixed in a 10% formaldehyde neutral buffer solution overnight, decalcified in a 10% EDTA solution (pH 7.4) for 2 weeks at 4°C and cut into paraffin embedded 4.5-micrometer section routinely. The deparaffinizerd sections were incubated by 0.3% hydrogen peroxide in methanol to block the endogenous peroxidase activity for 30 min at room temperature (RT). For PCNA IHC, sections were placed in 0.01M citrate buffer (pH 6.0) for 15 min in a microwave oven. For BrdU-IHC, the sections were rinsed in tripsin buffer and then incubated with 95% formamide in 0.15M sodium citrate at 70°C for 45 min for denaturalization of DNA. After blocking nonspecific staining with 0.5% casein for 20 min at RT, mouse monoclonal anti-BrdU antibody (Bu20a; DAKO) and mouse monoclonal anti-PCNA antibody (PC-10; DAKO) were applied to the specimens at dilution of 1:100. Immunostaining was carried out using LSB2 kit as described above.

Results

Light microscopic findings of PDL on extracted molar roots

PDL attached to the root surface of extracted teeth was not completely uniform in thickness. However compared to the width of normal PDL (Fig. 1a), about a half of PDL in width was on an average seen on the root surface as shown in Fig. 1b. The width of PDL decreased with the enzymatic digestion and no cells were seen on the surface of teeth after digestion for 110 min (Figs. 1c, 2a–c). There were no findings suggesting release of pulpal cells from a pulp chamber due to the enzymatic digestion even in the specimens at 110 min digestion (Fig. 1c). The finding was indicative that contamination of pulpal cells into each PDL-SP was not evident.

Scanning electron microscopic findings

Roots of the extracted teeth were covered by rough collagenous PDL tissues and exposure of cementum was not seen (Fig. 2d). With time of digestion, the surface of PDL became smoother (Figs. 2e–h). Although a few cells were seen on the root surface after 90 min digestion (Fig. 2h), no cells were remained on the root surface and cementum was completely exposed at 110 min digestion (Fig. 2i). This result indicated that the 110M-PDL-SP was enriched by root lining cells.

Proliferation of PDL subpopulations

Cultured PDL cells were spindle in shape (Fig. 3a) and there was no obvious morphological difference among culture cells of PDL-SPs except 100M-PDL-SP, which consisted of more polygonal cells (Fig. 3b). Fig. 4a shows the proliferation curve

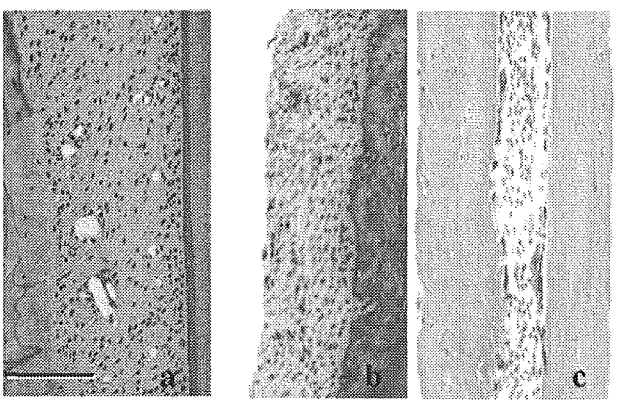

Fig. 1. Light microscopic features of PDL; normal PDL (a), before enzymatic digestion (b), and after 110 min digestion (c). About a half of PDL in width was seen on the root surface (b) compared to the normal PDL (a). No cells were seen on the root surface after digestion for 110 min (c). a–c: ×100, scale bar = 100 μm.

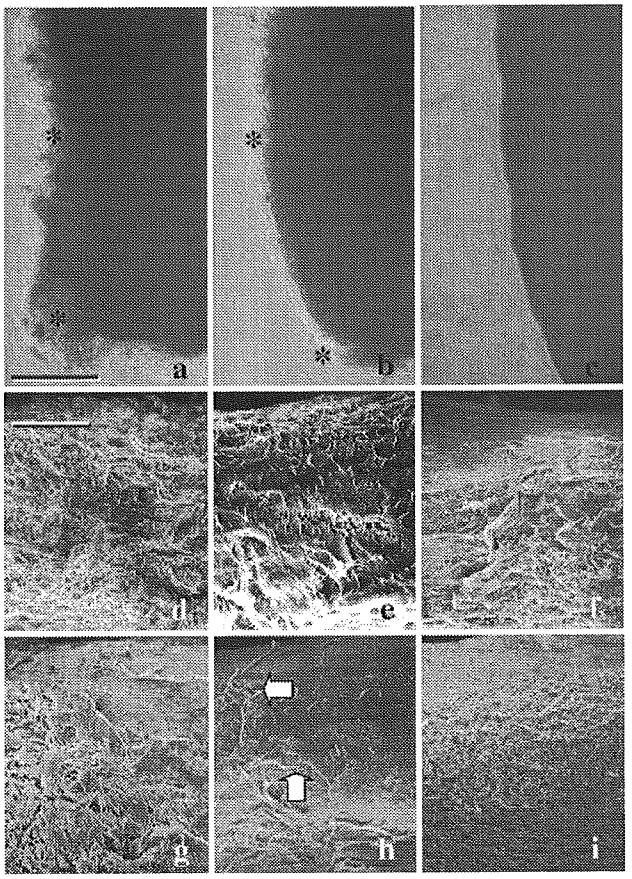

Fig. 2. Phase contrast microscopic features of PDL (*) before enzymatic digestion (a), after 70 min (b) and 110 min (c). The width of PDL decreases with the enzymatic digestion. No cells on the denuded root surface after 110 min digestion (c). a–c: ×100, scale bars = 100 μm. Scanning electron microscopic findings of periodontal ligament before digestion (d), after digestion for 30 min (e), 50 min (f), 70 min (g), 90 min (h) and 110 min (i). A few cells on the root surface (→) after 90 min digestion (h) are not seen after 110 min digestion (i). d–i: ×50, scale bar = 200μm.

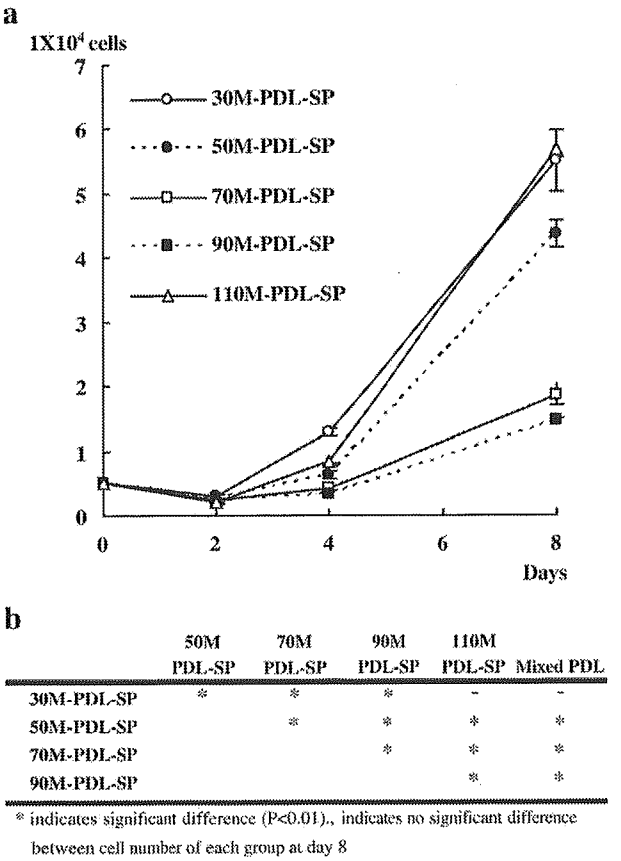

Fig. 4. Proliferation potential of periodontal ligament subpopulations (PDL-SPs) (a) and significant differences between each PDL-SP (b). 30M-PDL-SP shows a high level of a proliferative activity. Proliferative activity of PDL-SP decreases toward the root surface, 110M-PDL-SP, however, has high proliferative potential equivalent to that of 30M-PDL-SP (Mann-Whitney U-test: $P < 0.001$ versus 50-, 70-, 90-PDL-SP).

of each PDL-SP and Fig. 4b lists significant differences ($P < 0.05$) between each PDL-SP. 30M-PDL-SP, which was enriched by cells from middle portion of PDL, showed a high level of a proliferative activity. Although the proliferative activity of PDL-SP decreased toward the root surface, 110M-PDL-SP, which was enriched by cells on the root surface, had high proliferative potential equivalent to that of 30M-PDL-SP.

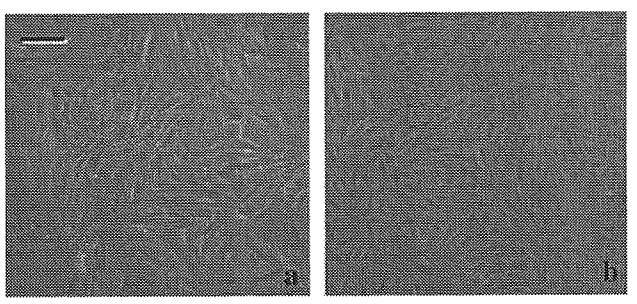

Fig. 3. Phase contrast microscopic features of 30M-PDL-SP (a) and 100M-PDL-SP (b). 30M-PDL-SP consists elongated spindle fibroblastic cells. In the culture cells of 110M-PDL-SP, a lot of more polygonal small cells (cementoblastic cell) were seen. a,b; ×150, scale bar = 33 μm.

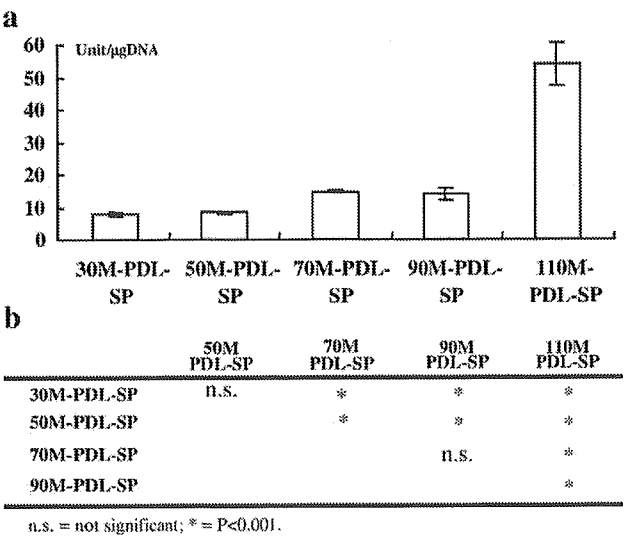

Fig. 5. Quantitative measurement of alkaline phosphatase (ALP) activities (a) of periodontal ligament subpopulations (PDL-SPs) and significant differences between each PDL-SP (b).